Hydrochemical evolution of high uranium, fluoride and nitrate groundwaters of Namakwaland, South Africa.

Sisanda S Makubalo[1] and Roger E Diamond[2]*

[1] Geological Resources Division, Council for Geoscience, Pretoria, South Africa smakubalo@geoscience.org.za

[2] Department of Geology, Faculty of Natural and Agricultural Sciences, University of Pretoria roger.diamond@up.ac.za ; * corresponding author

Highlights

Obtained a large dataset for the groundwater chemistry of Namakwaland.

Established that marine aerosol is the main contributor of major ions except Ca^{2+} and HCO_3^-.

Showed that high nitrate is from farm animals and high fluoride from geology and evaporative concentration.

Postulates evaporation and secondary mineral precipitation as two different processes responsible for uranium enrichment of groundwater.

Proposes that groundwater is usable with care in certain locations.

ABSTRACT

Water quality globally suffers from overuse and pollution, but desert areas with high evaporation rates and groundwater as the only water source have additional challenges. Namakwaland in the Northern Cape is an arid region with a sparse human population dependent largely upon stock farming, with minor mining and tourism. The complex Proterozoic metamorphic geology is overlain by Cenozoic deposits known for containing secondary uranium mineralisation in places. 86 samples of groundwater were taken over an area of 25 000 km^2 and analysed for various parameters in the field and laboratory. The salinity of the water varies from fresh to sea water, averaging 2500 mg/L, with pH in the 7-9 range. Major ion abundances indicate marine aerosol as the main source of Cl, Na, Mg and K, with rock weathering being more responsible for Ca and HCO_3. Irrigation water quality tests give mixed results, suggesting careful use of groundwater is possible in some locations. Nitrate is occasionally high, the random distribution indicating farm animals as the source. Fluoride averages 2.4 mg/L and is strongly geologically controlled, but

also enriched through evaporation. Uranium, averaging 0.155 mg/L (5 times the guideline), has a complex distribution, poorly correlated to bedrock geology and shows two enrichment trends, one in tandem with other ions and one independent. These two trends are proposed to reflect enrichment through evaporation (other ions also increasing) or precipitation of secondary uranium minerals (limited correlation with other ions). These three parameters are uncorrelated, which emphasizes the variety and complexity of hydrochemical processes taking place. Given the U and other water quality risks, further work into cumulative exposure for plants, animals and humans is warranted.

Keywords

groundwater, salinity, uranium, South Africa, Namakwaland

1 Introduction

Water resources globally are in a state of decline due to the expanding human population and increasing consumption of natural resources (Foster & Chilton, 2003). This decline manifests as reduced quantity of water leading to lowering of water tables (De Brito Neto et al, 2016) as well as reduced quality of water from pollution and excess evaporation (Kanyerere et al, 2012). The situation is no different in southern Africa, where groundwater resources are suffering depletion (Ebrahim et al, 2019) and pollution (Winde & Van der Walt, 2004). As a result, humans are resorting to ever more marginal land and water resources for various uses, including domestic and agricultural purposes (Gobin et al, 2019).

Desert areas worldwide may contain large fresh groundwater resources in certain basins, such as the Nubian Sandstone Aquifer in the north-east of Africa, but more often have poorer quality, saline groundwater, such as in Australia (Skrzypek et al, 2016) and Tunisia (M'nassri et al, 2019). Groundwater in the arid regions of southern Africa can also be moderately (Abiye & Shaduka, 2017) to highly saline (Molwalefhe, 2004) and may have additional quality challenges relating to a particular element or substance, such as fluoride (Abiye et al, 2018) or nitrate (Tredoux & Talma, 2006).

Using water with high salinity or particular dissolved species poses risks, whether for irrigation, stock watering or human consumption. Typical concerns are overall salinity, fluoride, nitrate, or metals, such as uranium. Saline water is unpleasant or poisonous to drink, can become toxic to plants or animals, especially with evaporation from the soil causing further concentration of salts, and causes permanent damage to soil, especially when sodium levels are relatively high (Ramesh & Elango, 2012). Fluoride is a critical nutrient for healthy bones and teeth, and when too low or high causes a variety of cosmetic to fatal health issues for bones and teeth (McGrady

et al, 2012). Nitrate is an extremely widespread contaminant, especially in densely populated areas, or areas with poor sanitation (Baloyi & Diamond, 2019), but it is also known to occur in high levels naturally in southern Africa (Tredoux & Talma, 2006). It is generally accepted that it is a health risk, but the evidence for this is not that clear and may not be as dangerous as is commonly believed (Manassaram et al, 2006). Uranium in water has a metal toxicity threat as well as a radiological risk (Banning et al, 2013). It occurs in elevated and potentially dangerous concentrations in groundwater in various parts of the world, such as India (Duggal et al, 2017) and Burundi (Post et al, 2017). Namakwaland is known to have surficial uranium deposits (Cole, 1998) and high levels of radioactivity have been reported in the groundwater (Abiye & Leshomo, 2013).

2 Aims

The main aim of this study was to document the groundwater quality in a region that is totally dependent upon groundwater. In addition, a subsidiary aim was to use hydrochemistry to understand hydrological processes, and specifically the evolution of groundwater quality in the region, with an emphasis on those dissolved species that pose potential health risks to humans, stock animals and the environment.

3 Study Area

The study area is situated in Little Namakwaland in the Northern Cape province of South Africa (Figure 1). Namakwaland is divided by the lower course of the Gariep (Orange) River into two portions — Little Namakwaland to the south, in South Africa, and Great Namakwaland to the north, in Namibia. The landscape of Little Namakwaland consists of two regions -- a western region of the north-south-trending Southern African escarpment, with rugged outcrops of basement gneisses in the form of tors and bornhardts, and an eastern region of subdued topography with very gently sloping plains and low gradient watercourses, with minor outcrop of varied geology in rocky hillocks. This latter, flatter subregion of Little Namakwaland is also known as Bushmanland.

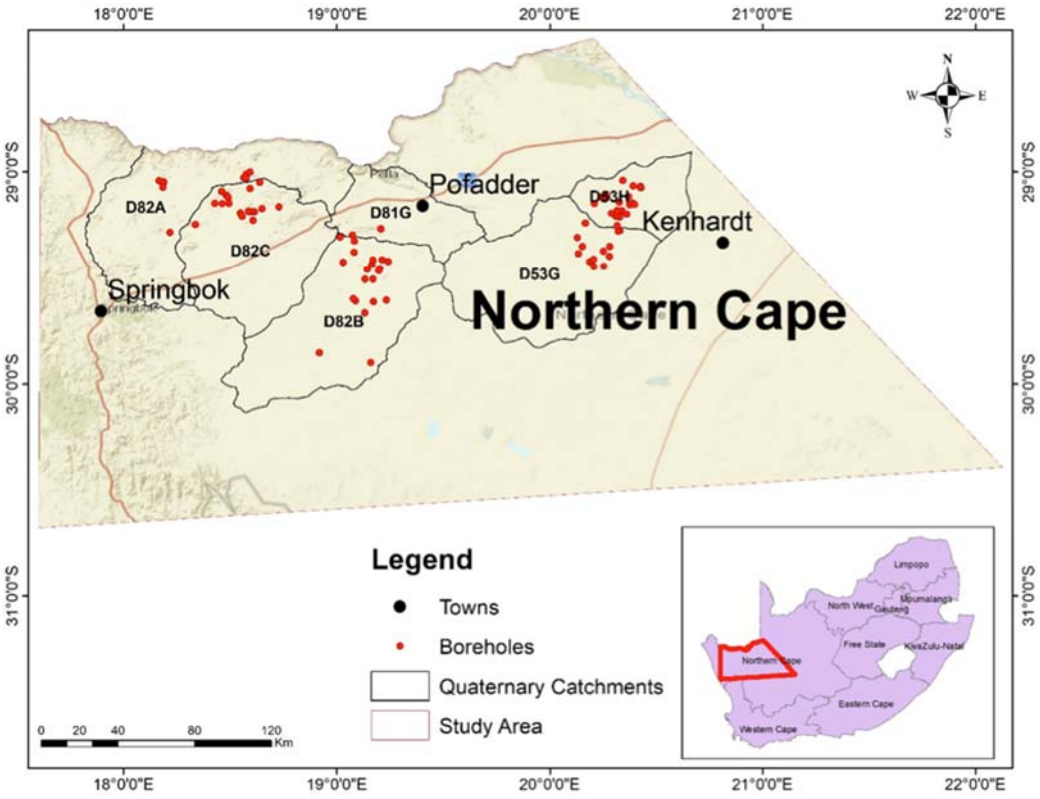

Figure 1. Map of the study area.

The basement geology of the area comprises rocks of the Namakwa-Natal Metamorphic Belt, subdivided into the Richtersveld and Bushmanland and other Subprovinces by Hartnady et al (1985), and later into terranes divided by structural discontinuities by Cornell et al (2009).

The older, Palaeoproterozoic Richtersveld Subprovince comprises a volcanosedimentary sequence metamorphosed to gneisses, amphibolites, schists and quartzites, onto which the younger, Neoproterozoic Bushmanland Subprovince rocks were intruded or deposited, comprising paragneisses, orthogneisses, amphibolites, psammo-pelitic schists, quartzites, calc-silicates and granitoids (Joubert, 1986; Bailie et al, 2007). Towards the south and east, these rocks are overlain by the Mesozoic Karoo Supergroup, which in the study area consists of clastic sedimentary rocks of the Dwyka Group, comprising mainly tillite, and Ecca Group, comprising varied clay and sand rich rocks of marine genesis. These, and the older rocks, are intruded by sills and dykes of Jurassic dolerite, part of the igneous event that terminated the Karoo basin deposition (Blignaut et al, 1983). All of this is mostly covered by variable thicknesses of Cenozoic sediments, made up of alluvium, calcrete, pan sediments, calcareous and gypsiferous soil, and red and grey aeolian sand. Calcrete is confined mainly to topographic highs of the Bushmanland Plateau adjacent to the Koa River Valley and, further east, occurs as scattered nodules and irregular layers within various superficial sediments (Figure 2).

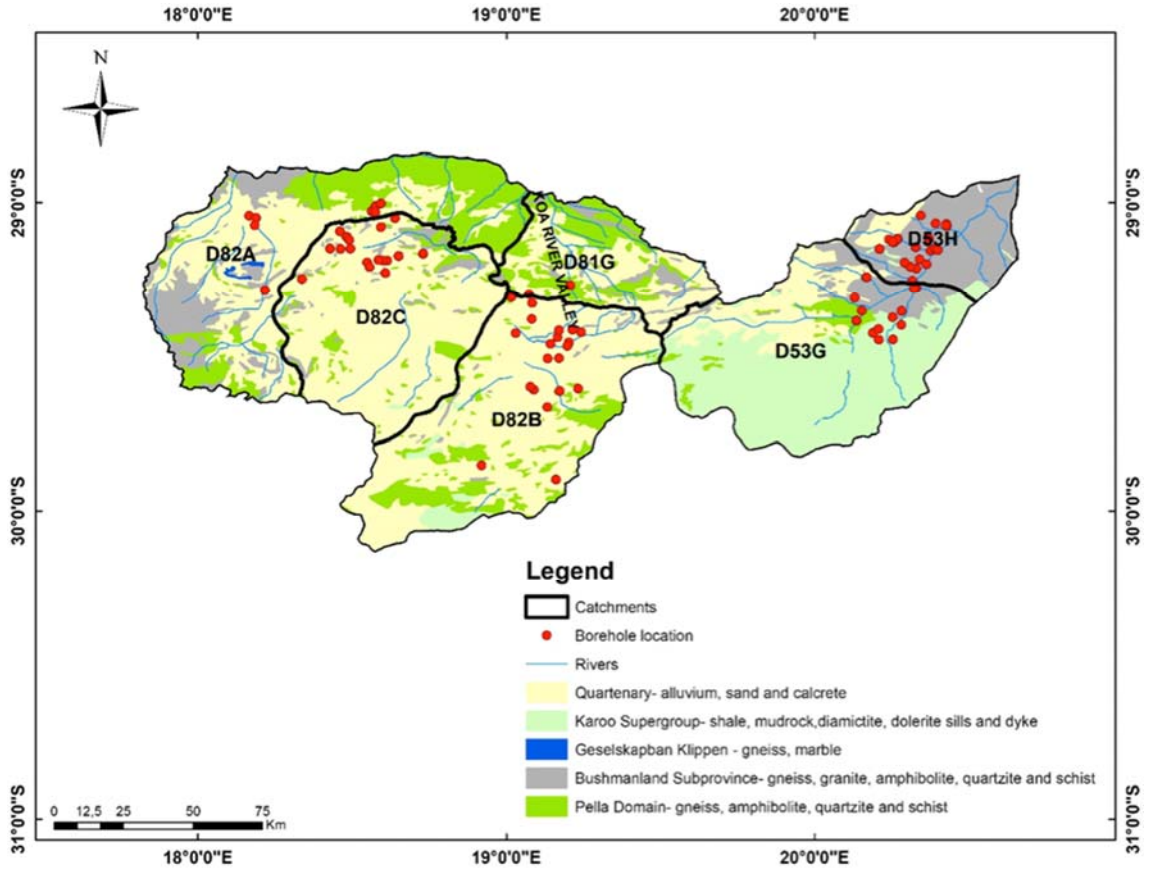

Figure 2: Surface geology of the study area, with Quaternary catchments shown (modified from Macey *et al*., 2018).

The area is arid to semi-arid, with the mountainous areas receiving higher rainfall than the lowlands due to orographic effects (Olivier and Van Heerden, 1999). Rainfall in Namakwaland is characterized by two pronounced geographical rainfall gradients (Desmet and Cowling, 1998). The first is a gradual latitudinal aridity gradient with the overall precipitation decreasing as one moves northwards into the southern Namib Desert. The second is a shift from winter rainfall in the west, closer to the coast, to summer rainfall further east and inland. Precipitation ranges from 50–400 mm per annum and is highest over the Kamiesberg Mountains (1706 m) near Garies, south-west of the field area. More rain occurs in Little Namakwaland in the winter months, from May to September, due to the westerly cold fronts from the Atlantic Ocean. Heavy dewfall, related to advection from coastal fogs, increases the amount of precipitation (Davis *et al*, 2016). Large variations between maximum and minimum temperatures, both on daily and seasonal cycles, characterize the region and daily mean temperatures range from 13–26 °C through the year. The potential evaporation of the area exceeds 2000 mm everywhere, but decreases from west to east. The mean annual potential evapotranspiration exceeds the mean annual precipitation everywhere in the study area. This results in the formation of evaporitic salts at the surface and in the subsurface (Nakwafila, 2015).

Watercourses are emphemeral and flow only after heavy rain that occurs once every several years. The hydrogeology is not well understood, but there are three possible types of aquifer in the region. These are fractured bedrock, the weathered zone and the unconsolidated Cenozoic deposits of alluvial, colluvial and aeolian genesis. The latter is probably the highest yielding of the three, but the underlying geology, including the structural properties of the bedrock, control and influence the geometry and water flow in the overlying weathered and transported materials (Pietersen et al, 2009). Importantly however, these different stratigraphic units probably behave as a single hydraulically linked aquifer, and can be thought of as a single hydrostratigraphic unit (Adams et al, 2004; Diamond et al, 2019).

The most important economic activities in the area are livestock farming (sheep and goats), crops (mainly grapes), with some mining and tourism.

4 Methods

85 groundwater samples were collected from six Quatenary catchments from boreholes currently used for human and animal consumption in the Little Namakwaland area in July 2017. Samples were collected in polyethylene bottles of 500 ml capacity. Prior to filling with sample water, these bottles were rinsed with distilled water to minimize potential contamination. The sampling procedure and preservation was based on the comprehensive guide for groundwater sampling methods by Weaver *et al*., (2007). Field measurements of temperature (T), electrical conductivity (EC), pH, oxidation-reduction potential (Eh) and dissolved oxygen (DO) were made for each borehole, using Extech ExStik® handheld probes. In addition, the probes automatically calculated the total dissolved solids (TDS) and salinity. Sample bottles were immediately placed into a cooler box with ice and transferred to a refrigerator daily until being transported to the laboratory.

In the laboratory, cations and trace elements were analysed using a Perkin Elmer ELAN® DRC II inductively coupled plasma mass spectrometer. Anions were analysed with a Thermo Gallery Plus discrete analyser and alkalinity with a Metrohmn 854 autotitrator. Laboratory quality control techniques of standard operating procedures, calibration with standards, and analysis of replicates and blanks, were applied to guarantee data quality.

Hydrochemical classification, groundwater evolution and groundwater examination of fitness for human and animal use have been discussed using a Piper plot, spatial distribution diagrams and scatter plots. For drinking water quality assessment, the results were compared with the South African National Standard (SABS, 2001) and World Health Organization standards (WHO, 2011). Various irrigation water quality parameters such as salinity hazard, sodium adsorption ratio (SAR), soluble sodium percentage (SSP) and Kelly's ratio (KR) were calculated from the hydrochemistry data (Todd 1980; Hem 1985).

5 Results

5.1 pH and Salinity

Groundwater in the study area is neutral to alkaline, with pH values ranging from 7.1 to 8.9. Most water samples fall within the ideal range for pH of 6–9 (SANS, 2001). EC however, ranges from 22 (borehole SSM031) to 1440 mS/m (SSM035), with an average of 350 mS/m. These values translate into TDS of 315–9980 mg/L, with an average of 2450 mg/L, where ideal levels for drinking are considered to be < 450 mg/L, and the maximum allowable level for health purposes is 2400 mg/L (SANS, 2001). As a result, 80% of the groundwater is of an undesirable nature for human consumption, and 45% is a health risk. One sample, SM032, was so salty that an EC reading could not be made with the field probe and therefore no TDS measurement is recorded. However, the sum of cations and anions from laboratory analyses show that SM032 has a TDS of over 34800 mg/L, which is roughly the salinity of the oceans (3.5%). The high TDS values are mainly caused by high levels of Na^+, Cl^- and SO_4^{2-} ions, with moderate levels of Ca^{2+} and alkalinity (HCO_3^-). These results are not surprising, given the presence of salt pans in the landscape, a sure sign of elevated salinity. These and other results are shown in Table 1. The TDS results are displayed geographically in Figure 3. Appendix A contains all the raw data.

Table 1. Summary statistics for the hydrochemistry, and exceedances of the South African National Standard (SABS241: 2001) guidelines, using the "maximum allowable" limit. Note that SM032 was so salty the field probe did not record an EC and TDS value, hence the maximum and mean EC and TDS values are calculated without this sample, and some maximum individual ion values (Cl^- and Na^+, both from SM032) exceed the maximum TDS. * WHO(2011) drinking water limit used as there is no SANS value.

parameter	units	n	minimum	maximum	mean	standard deviation	SANS max. limit	n > SANS max. limit
T	°C	85	7	28	18	5		
pH		85	7.1	8.9	7.7	0.40	4-10	0 (0%)
EC	mS/m	85	22	1443	350	150		
TDS	mg/L	84	315	9980	2450	1640	2400	38 (45%)
Na^+	mg/L	86	85	12800	911	1450	400	58 (68%)
Mg^{2+}	mg/L	86	14	329	70	53	100	15 (17%)
K^+	mg/L	86	2.3	133	21	20	100	1 (1%)
Ca^{2+}	mg/L	86	49	926	256	171	300	28 (33%)
Cl^-	mg/L	86	114	16500	1300	1900	600	58 (68%)
HCO_3^-	mg/L	86	0	740	294	163		
SO_4^{2-}	mg/L	86	11	3800	608	508	600	38 (45%)
NO_3^-	mg/L	86	0	299	51	52	90	17 (20%)
F^-	mg/L	86	0	5.9	2.4	1.0	1.5	73 (85%)
U	μg/L	86	1.3	5100	155	540	* 30	* 76 (88%)

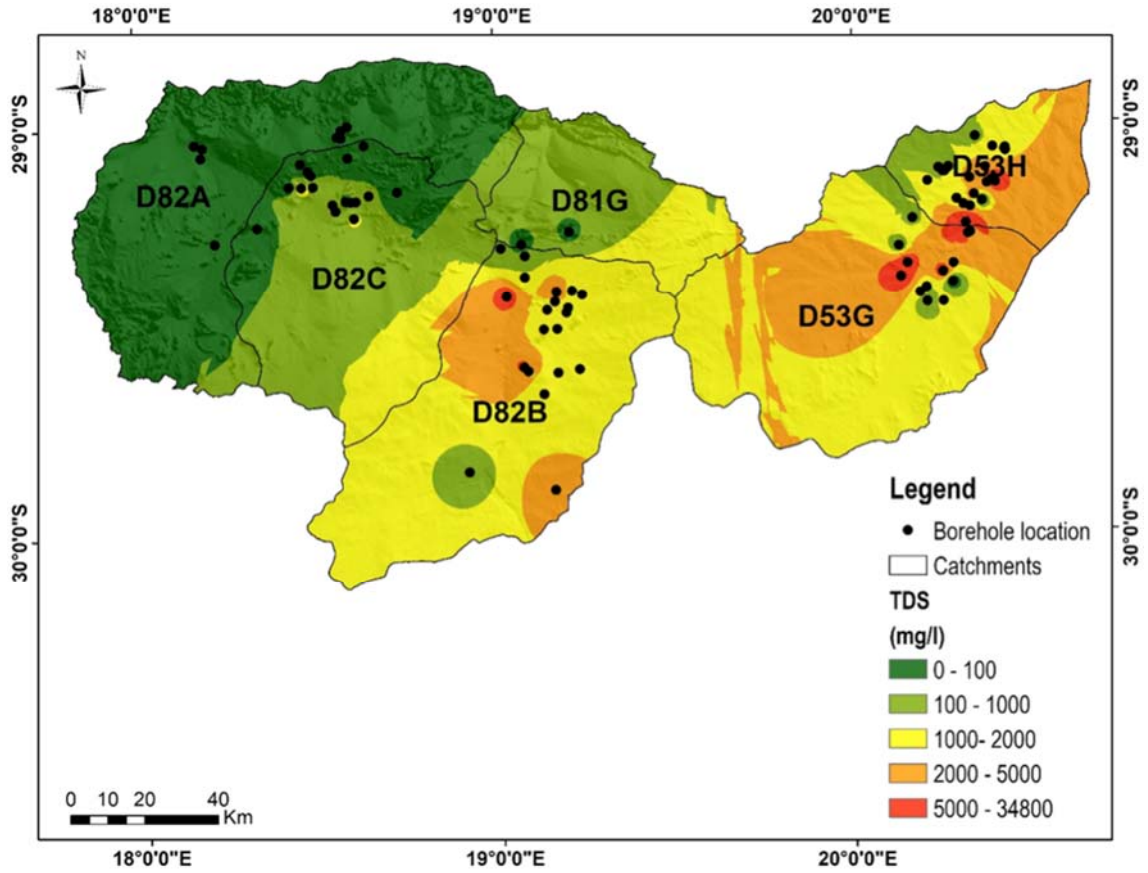

Figure 3: Spatial distribution of TDS (total dissolved solids) in the groundwater.

5.2 Irrigation Suitability

The quality of water for irrigation is determined by how long term use of water affects soil and plant health and the potential for reduced crop yields (Ramesh & Elango, 2012). Parameters typically used to assess the quality of water for irrigation include the salinity index (or EC), the permeability index (PI), the sodium absorption ratio (SAR), the soluble sodium percentage (SSP) and Kelly's ratio (KR). The last three parameters all relate to the sodium content or fraction.

5.2.1 Electrical Conductivity (EC)

EC is a direct measurement reflecting the salinity level of water, which is the primary indicator of water quality and usability. Saline conditions severely limit the choice of crop, adversely affecting crop germination and yields and can make soils difficult to work. High salinity can also lead to physiological drought conditions and ion toxicity (Zhu, 2002). Wilcox (1955) classified water into different classes based on the EC - see Table 2. The EC of groundwater in the study area varies from 22 to 1443 mS/m with an average of 350 mS/m. There are high values of EC in the Koa River drainage system and this is regarded as a groundwater discharge area, with high salinity being caused by the high evaporation and low gradients of Namaqualand (Levin, 1983)

.

5.2.2 Sodium Adsorption Ratio (SAR)

SAR (Richards, 1954) is an irrigation water quality parameter used in the management of sodium affected soils, because sodium concentration can reduce the soil permeability and soil structure (Todd, 1980). Sodicity in irrigation water is due to a high concentration of Na^+ relative to Ca^{2+} and Mg^{2+}. Application of irrigation water with high SAR to soil over several years can shift the calcium and magnesium out of the soil as they get exchanged for sodium coming from the water (Kumar *et al.,* 2009). This causes a decrease in the ability of the soil to form stable aggregates, a loss of soil structure and tilth and a decrease in infiltration and the permeability of the soil to water, leading to problems with plant growth, including crop production or land rehabilitation.

5.2.3 Combined EC-SAR Hazard Assessment

In a "Wilcox Diagram" (Figure 8), the EC on the x-axis is taken as the salinity hazard and SAR on the y-axis as the sodium hazard, with the results for this study giving a low-medium salinity hazard (C1-2) and low-high sodium hazard (S1-3) for the majority of groundwater samples. However, five samples (SM003, SM025, SM025A, SM027, SM035 and SM037) fall into C3 and S3-4 which represent high hazard ratings.

5.2.4 Other irrigation suitability ratings

Table 2 also contains two other irrigation suitability ratings, namely Kelly's Ratio (KR) and the soluble sodium percentage (SSP). These both confirm the general observation that the groundwater of the region varies widely in quality, with some usable for agriculture, but a lot that is marginal to poor in quality.

Table 2: Classification of groundwater for irrigation use on the basis of EC, SAR, KR and SSP.

parameter	formula & source	units	range	water class	% samples
EC (electrical conductivity)	--	mS/m	0-250	excellent	36
			250-750	good	60
			750-2250	permissible	4
SAR (sodium absorption ratio)	SAR = Na ÷ √((Ca+Mg)÷2) concentrations in meq/L (Richards, 1954)	--	0-10	excellent	56
			10-18	good	28
			18-26	doubtful	10
			>26	unsuitable	6
KR (Kelly's ratio)	KR = Na ÷ (Ca+Mg) concentrations in meq/L (Kelly, 1963)	--	<1	suitable	19
			1-2	marginal	49
			>2	unsuitable	32
SSP (soluble sodium percentage)	SSP = ((Na + K) ÷ (Na + K + Mg + Ca)) x 100 concentrations in meq/L (Doneen, 1964)	--	<50	suitable	19
			>50	unsuitable	81

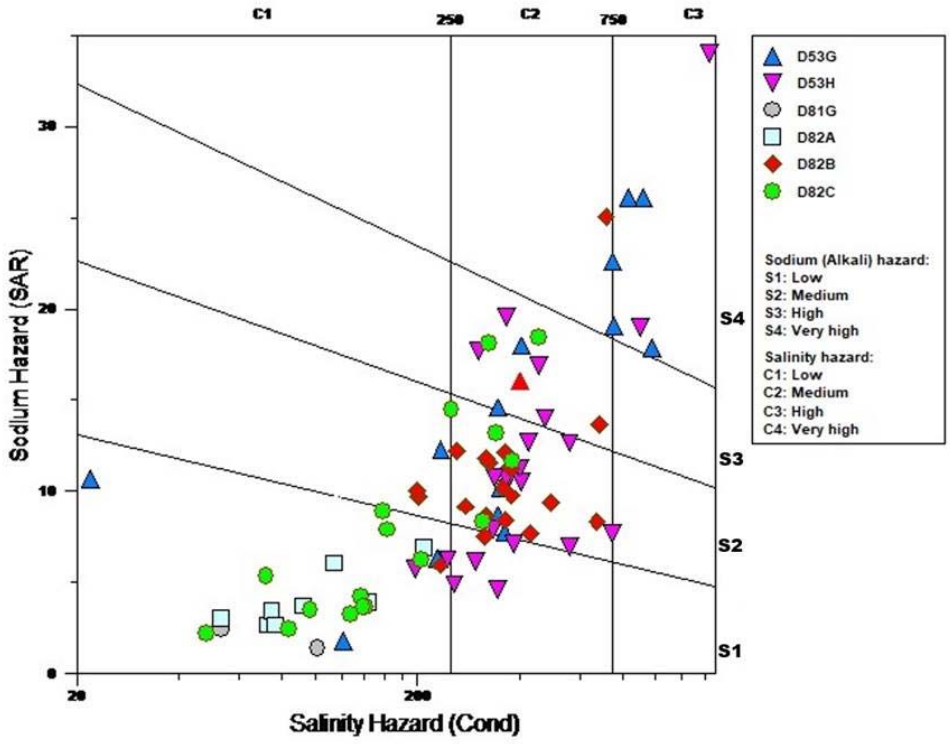

Figure 4: Classification of groundwater, coded by catchment, based on the Wilcox diagram, with EC (mS/m, conductivity) displayed logarithmically on the x-axis and the sodium absorption ratio (SAR) on the y-axis.

5.3 Major Ion Hydrochemistry

The distribution of major ions in the groundwater is as follows:

for cations: $Na^+ > Ca^{2+} > Mg^{2+} > K^+$

for anions: $Cl^- > SO_4^{2-} > HCO_3^- > NO_3^-$.

The acceptable range for Na^+ is ≤ 400 mg/L (SANS, 2001). Na^+ in the study area varies from 84 to 12800 mg/L, with an average of 908 mg/L (Table 1, Figure 5). As a result, 68% of samples exceed the target range. Figure 6 shows the spatial distribution of Cl^-, and it can be seen that this has a great similarity to the Na^+ concentrations shown in Figure 5. Cl^- concentrations range from 114 to 16 500 mg/L, with a mean of 1300 mg/L, and as with Na^+, 68% of samples exceed the SANS (2001) maximum allowable limit of 600 mg/L Cl^-.

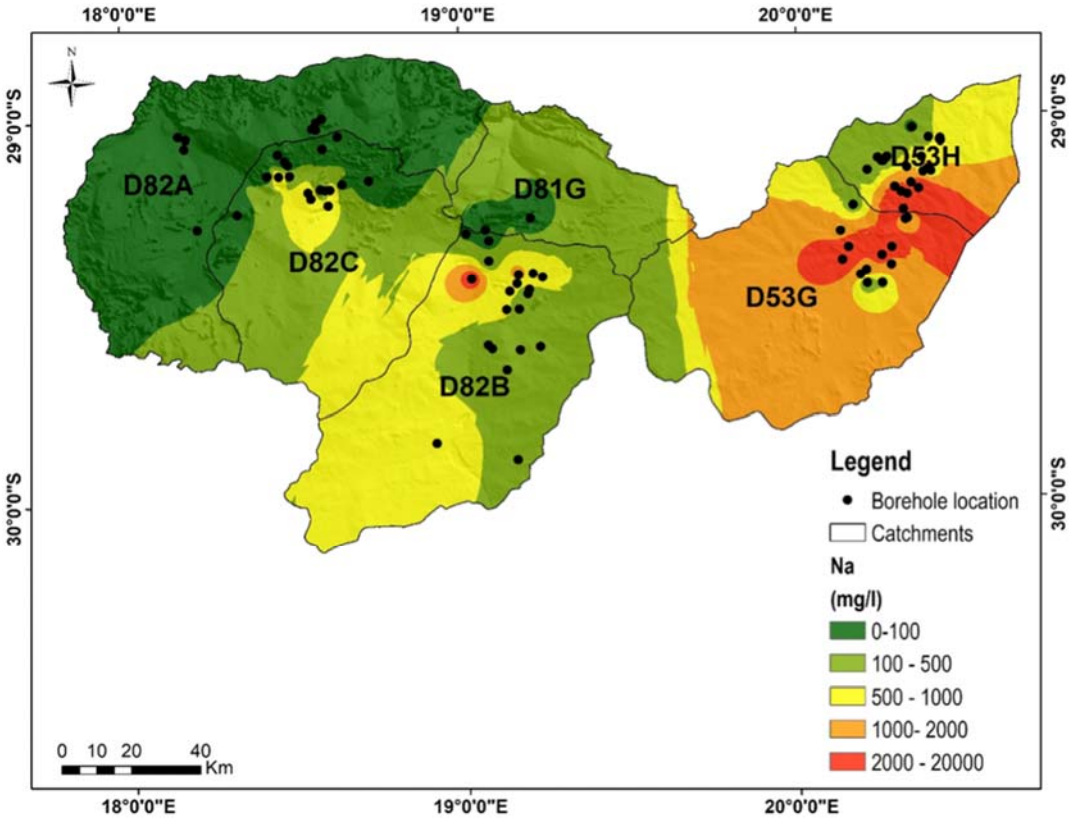

Figure 5: Spatial distribution of sodium (Na^+) in the groundwater.

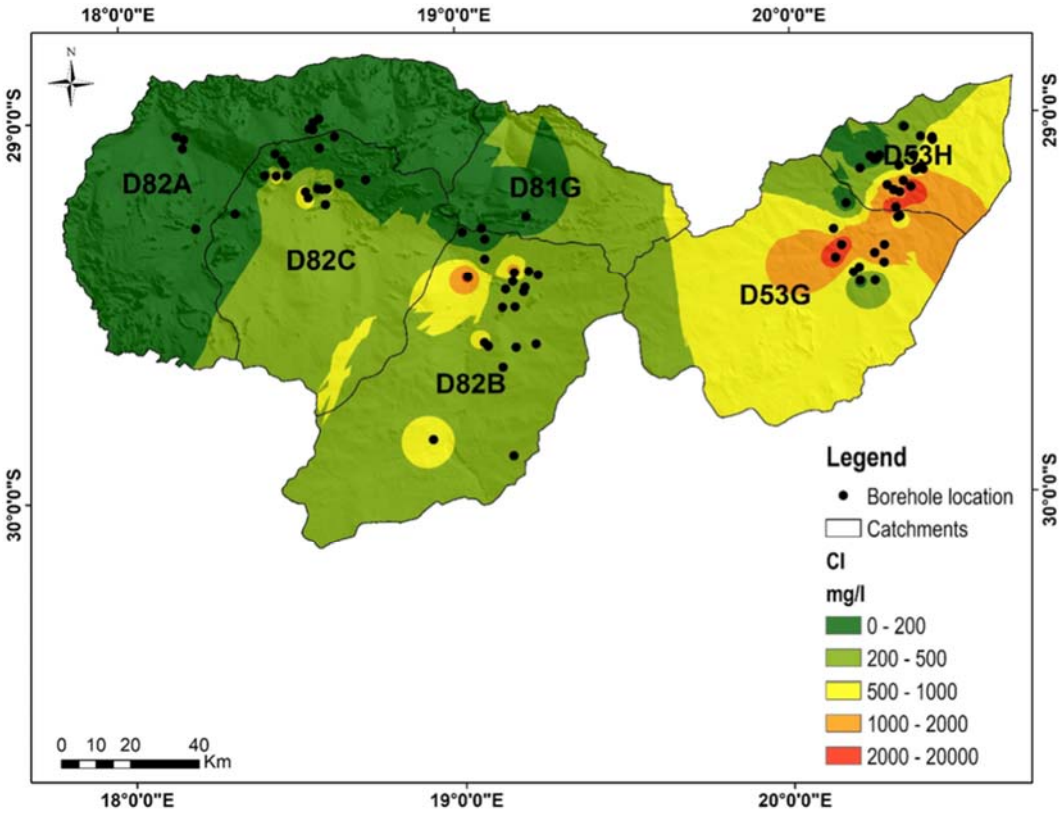

Figure 6: Spatial distribution of chloride (Cl^-) in the groundwater.

The results of similar analyses of the data for the other major ions and some relevant minor or trace constituents is shown in Table 1. Due to the fact that the WHO values are conservative and represent levels that "...do not represent any significant risk to health over a lifetime of consumption, including different sensitivities that may occur between life stages." (WHO, 2011, p1), the SANS "maximum allowable" limit was chosen, so exceedance of this amount is more likely to cause some sort of health issue. However, the actual levels at which health impacts occur is so variable, due to degree of exposure (intensity) and duration of exposure, as well as confounding factors, such as diet, lifestyle and genetics.

A Piper plot (Figure 7) was constructed, using AQUACHEM software, to understand the water composition within the study area. Based on this, the predominant water type in the study area is Na-Cl, verging somewhat towards Ca-HCO_3. The Na-Cl water dominates catchment D53H, gradually becoming Ca-HCO_3 richer in catchments D53G, D82B and D82C. See Figure 6 for the distribution of Cl^- in the study area. Most of the sampled water in the study area has a Na-Cl water type, coming from boreholes mainly distributed in Cenozoic sediments in contact with granites, gneisses and quartzite. The Na-Cl water type dominates in the areas that also have higher values of TDS. Catchments D53H and D53G are located in the Sout River. The groundwater salinity is closely related to the surface water quality (when surface water is present), as the name of the river (Sout River) and presence of salt pans attest.

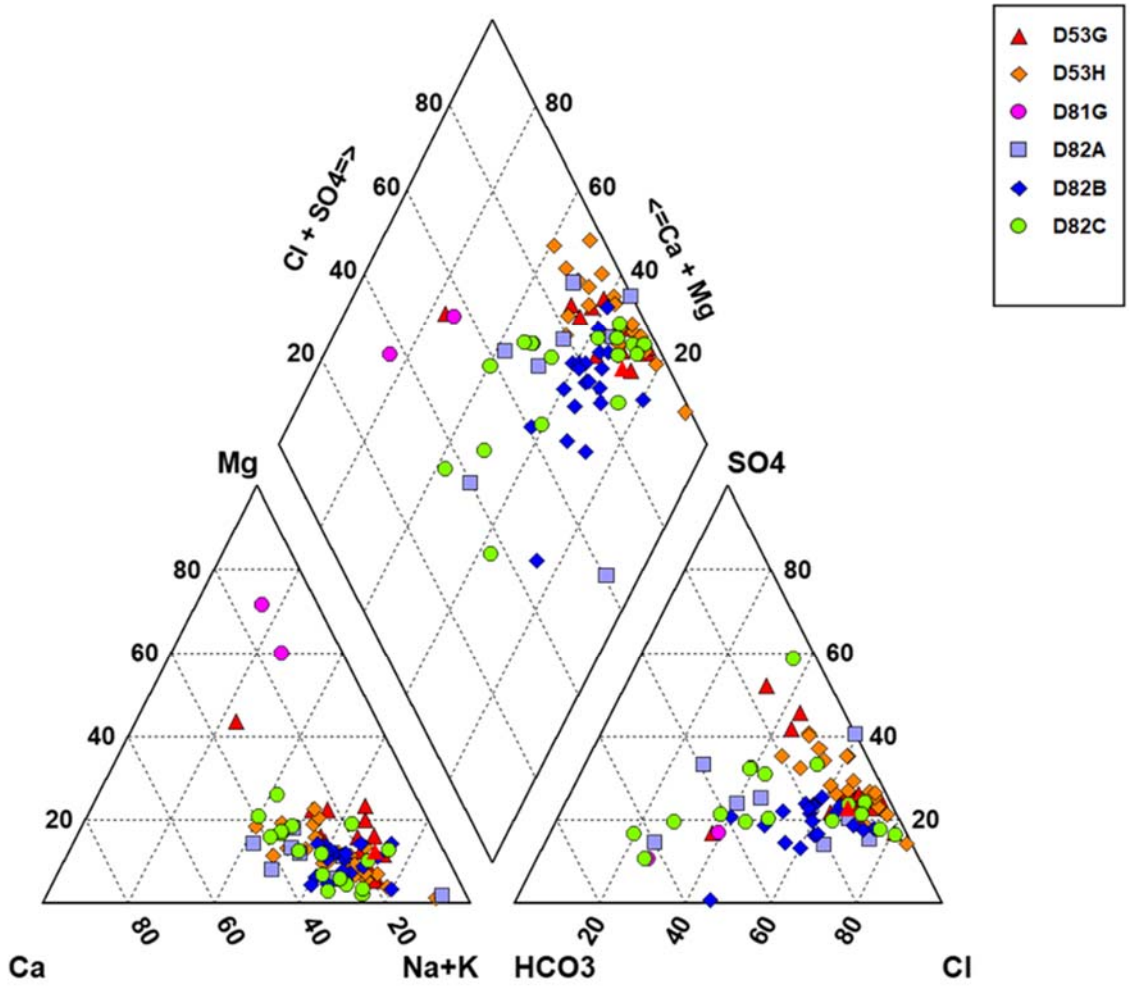

Figure 7: A Piper plot of all groundwater samples, coded by catchment.

Mg tends to be very low, except for 3 samples, two of which are the only samples from catchment D81G (Figure 7). These samples are very fresh water (see the TDS values in Figure 3) and occur in the Gariep River valley, where topographic drive will keep most groundwater young and therefore fresh. The predominance of Mg^{2+} and relatively higher HCO_3^- is evidence for rock weathering, and particularly of mafic or ultramafic rocks. This area contains amphibolite (Figure 2) and other metapelitic rocks, so will have a higher abundance of magnesium than the felsic igneous rocks or younger sediments and sedimentary rocks dominating elsewhere in the region.

The three catchments D82A-B-C all display a variation in the Cl-HCO_3 values, suggesting the influence of rock weathering (producing HCO_3^-) is variable in these areas. In contrast, catchments D53G-H show a more consistent Cl-SO_4 signature, suggesting less input of ions from freshly weathered rock. These observations are in line with the landscape, where catchments D82A-B-C are in the gently sloping Gariep River valley and have fresher groundwater due to the faster throughflow (Figure 3), resulting in less time for evaporative enrichment of Cl^- and hence

the existence of more HCO_3^- rich waters. Catchments D53G-H are in the very low gradient Sout River landscape, where throughflow is rare, and evaporation has therefore concentrated the dissolved ions into more saline water (Figure 3) with a more marine signature.

Figure 8 shows the major cations (Na^+, Mg^{2+}, K^+, Ca^{2+}) relative to chloride. Several patterns are interesting. Firstly, there is generally a good correlation between all the cations and Cl^-, indicating that the bulk of dissolved matter is from marine aerosol, because all Cl^- is ultimately sourced from the sea, as there are no geological sources of Cl^- in this region. Increased amounts of Cl^- are from evaporative enrichment. This excellent correlation between Na^+ and Cl^-, and the closeness to the sea water line is further evidence for this. The additional Na^+, over and above the sea water line, is from addition of Na^+ through rock weathering, specifically plagioclase in the igneous and metamorphic rocks underlying the region. Ca^{2+} displays an excellent correlation with Cl^-, however in quantities well above the sea water ratios. There are two possible processes causing the excess abundance of Ca^{2+} over the sea water line. The first is release of Ca^{2+} from rock weathering, and the second is where Ca-bearing minerals precipitate and remain in the catchment, but chlorides stay soluble and are washed out of the catchment. In other words, both Ca^{2+} and Cl^- increase over time with successive cycles of evaporative enrichment, but Ca^{2+} moreso, as it is less soluble than Cl^- and there is a steady contribution over time from rock weathering.

Both Mg^{2+} and K^+ show poorer correlations, due to scattered points of higher Cl^- samples showing relatively low Mg^{2+} and K^+ compared to the sea water line. These are only a few samples, so could be a random error effect, but may also be due to the very high solubility of Mg- and K-salts. In cases of extreme evaporative enrichment, where most Cl-salts are depositing (NaCl mainly), the so-called bittern salts (containing Mg^{2+} and K^+) remain in solution and get removed from the catchment, thus lowering the levels of these cations relative to the sea water line (Femitha & Vaithyanathan, 2013). There are also samples with relatively more of these cations than Cl^-, and this is likely simply due to rock weathering of various minerals adding cations (and bicarbonate) to the water.

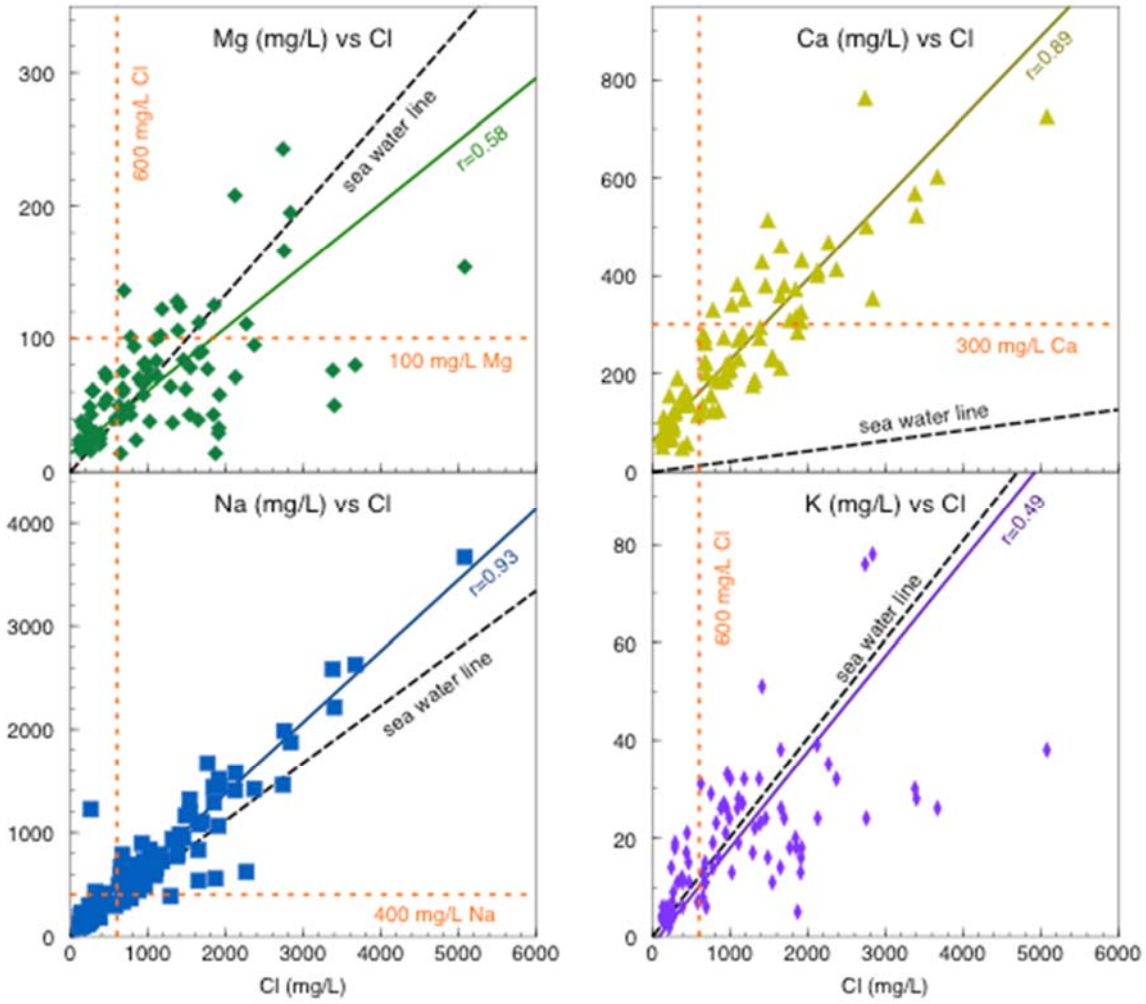

Figure 8: Scatter plots of major cations versus Cl^-. Solid colour lines are structural regressions, with the Pearson's r correlation coefficient indicated. The dashed black "sea water line" shows the relative ratios of these ions that would be present in sea water at any concentration (in essence, a mixing line between sea water and pure distilled water). The SANS (2001) drinking water guideline limits are also shown, as orange dotted lines. Data for SM032 is not displayed, as it is an extreme outlier and would relegate all other points to a small fraction of the graphs.

5.4 Trace element hydrochemistry

The samples were analysed for a wide suite of minor and trace dissolved elements. Of particular interest for health reasons are the fluoride values (Figure 9). Ranging from 0 to 5.9 mg/L with a mean of 2.4 mg/L F^-, where the SANS (2001) limit is given as 1.5 mg/L, high fluoride is clearly a health risk, as 85% of samples are above this limit.

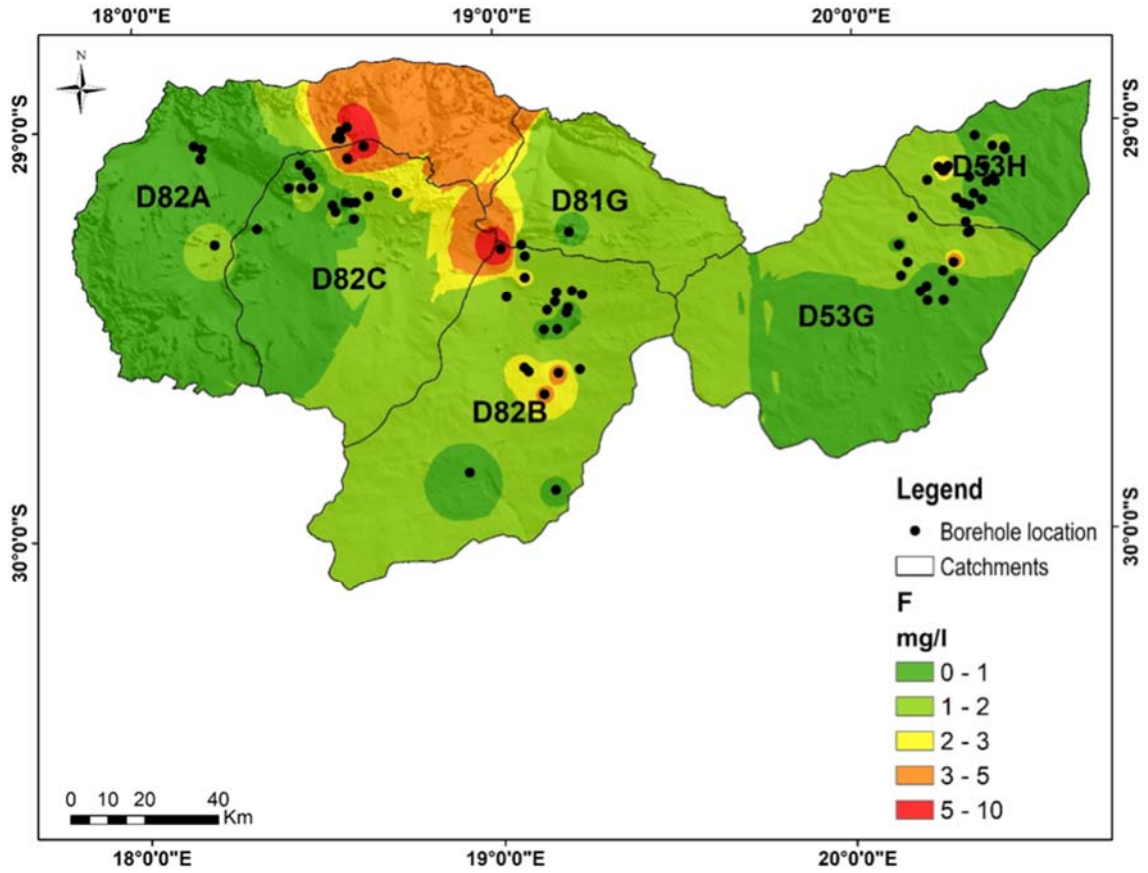

Figure 9: Spatial distribution of fluoride (F^-) in the groundwater.

Nitrate, although not strictly a trace element in a geochemical sense, is a minor constituent of groundwater with health implications, both for human and animal consumption, as well as environmental reasons, and so is considered here. NO_3^- is found from 0-299 mg/L, averaging 51 mg/L, and exceeds the SANS (2001) maximum allowable limit of about 90 mg/L in 20% of cases (Figure 10).

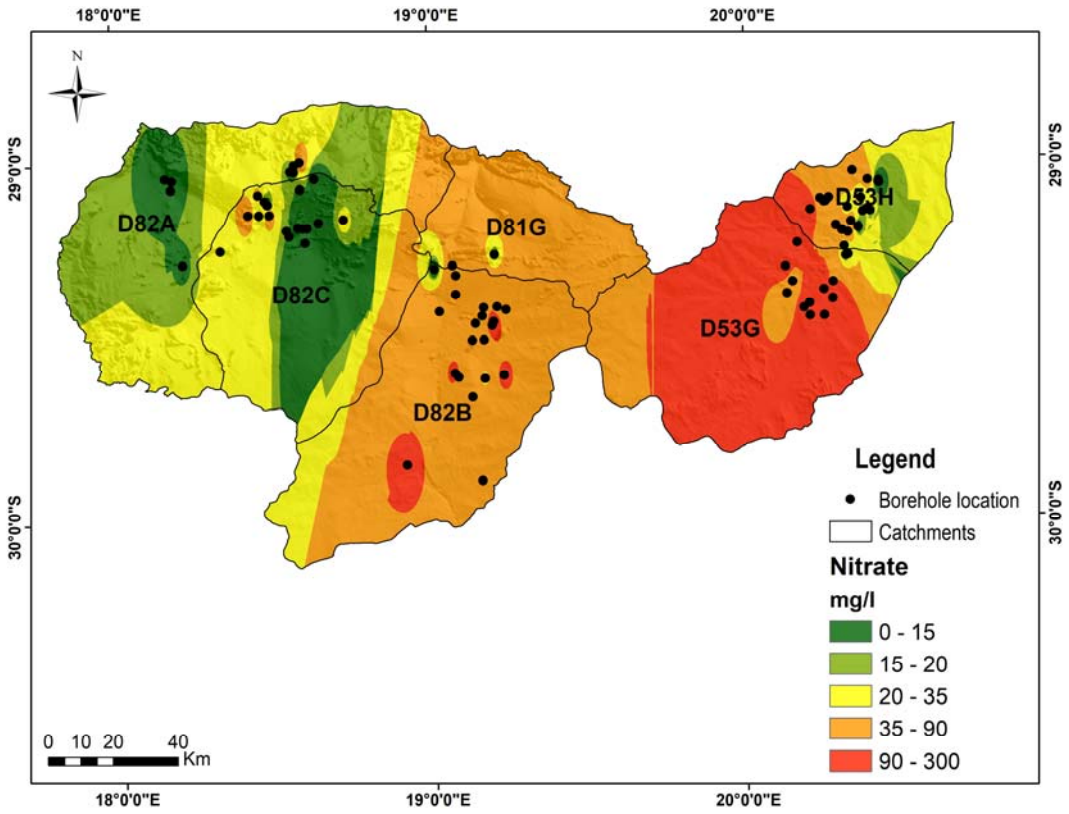

Figure 10: Spatial distribution of nitrate (NO_3^-) in the groundwater.

Uranium is extremely enriched in the groundwater of the study area. As seen in Table 1 and Figure 10, only 12% of samples fall below the WHO (2011) guideline value of 30 ug/L. The mean is 155 μg/L, which is more than 5 times the limit. However, there is a single extremely high value of 5120 μg/L from the same borehole that contains most of the outlying high values of dissolved species (SM032). The median would therefore be more instructive, but even the median for U is 76 μg/L, which is more than double the WHO (2011) limit.

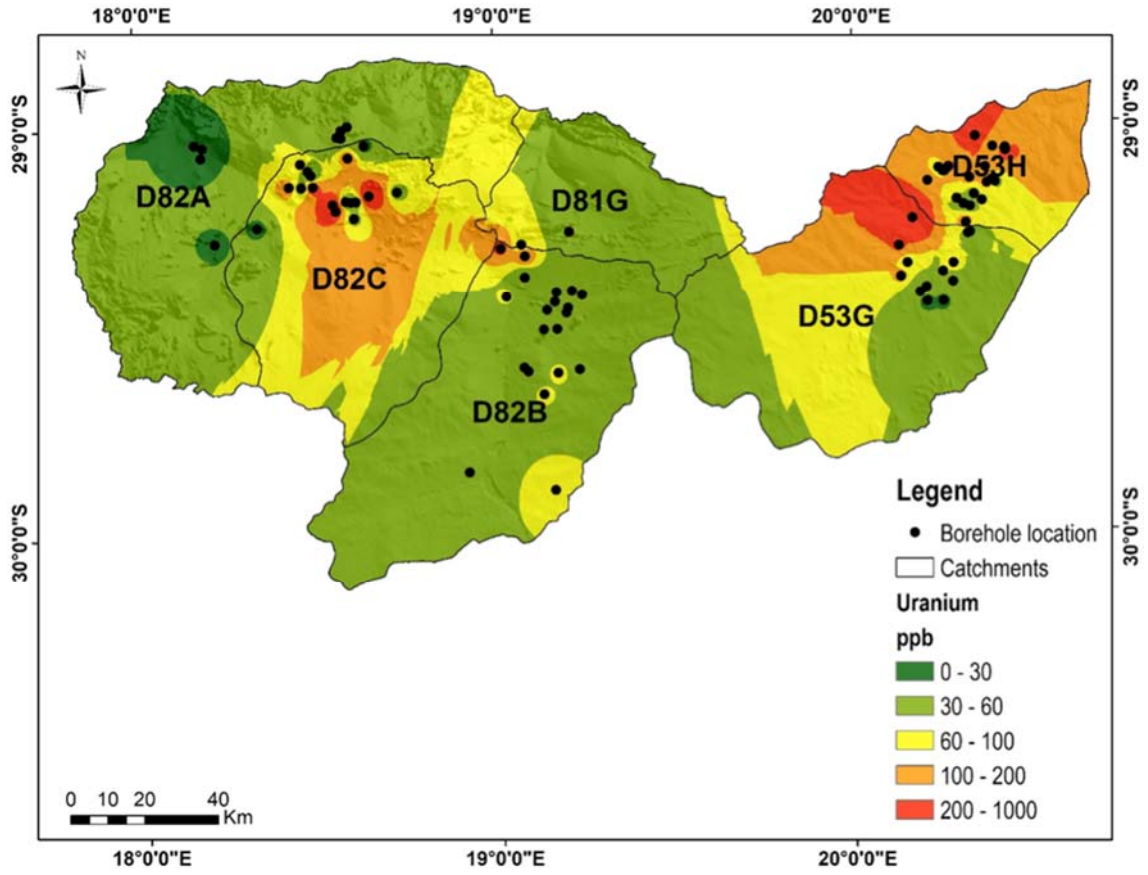

Figure 11: Spatial distribution of uranium in the groundwater.

6 Discussion

The discussion focuses on F^-, NO_3^- and U, as they occur at elevated levels and have health implications. They also reveal different aspects of the hydrochemistry. These three parameters are not correlated and so the discussion deals with each one separately.

The study area generally contains high F^- in the groundwater, but particularly dangerous F^- levels (> 3 mg/L) are restricted to a few areas, most of which lie on or near rocks of the Pella Domain of the Namaqua-Natal Metamorphic Belt (Figures 9 & 2). Sample SM067 shows the highest concentration of F^- (5.9 mg/L) and this borehole is located in the Stalhoek Complex leucocratic biotite gneiss. High F^- levels are known from various parts of South Africa (Ncube & Schutte, 2005) and are well correlated with dental fluorosis (Odiyo & Makungo, 2012) where teeth become mottled, malformed and brittle. Hydrogeological explanations for the high F^- found in the groundwater of Namaqualand include source rocks of felsic igneous type, alkaline groundwater with high EC (750-1750 mS/m) (Abiye & Leshomo, 2013), evaporative concentration and long residence time, as confirmed to some degree by tritium levels below 1.7 TU (Abiye et al, 2018). The last two terms are in turn caused by low topographic gradients and low rainfall, both of which

contribute to slow groundwater movement and ample opportunity for evaporation. Similar reasons are given for high F^- concentrations in groundwater elsewhere in the world (e.g. Krishan et al, 2017).

Analysis of F^- with other hydrochemical parameters reveals no correlations. This suggests that a single, simple geochemical process is not responsible for the distribution of F^- in the region. It is likely that a combination of source rock type and subsequent controls on mobility in groundwater are giving rise to the distribution observed. This disagrees with some of the previous conclusions given by Abiye & Leshomo (2013) and Abiye et al (2018) for this region, who gave evaporative concentration, long residence time and alkaline groundwater with high EC as reasons for high F^-. This study did not find any correlation with EC, HCO_3^- or other ions (Na^+, Cl^-, etc) to suggest evaporative concentration or long residence time are important processes. Given these conflicting findings, further work would be required to reveal the processes determining F^- distribution. We suspect not only the complex geology, but also the variety of landforms and differing land uses contribute to the range of hydrochemical processes acting on F^- distribution.

NO_3^{2-} ranges from undetectable to almost 300 mg/L, averaging 51 mg/L, with 38% of samples over the 50 mg/L WHO (2011) guideline limit. There is no correlation with any other parameter, which suggests a different process responsible for NO_3^{2-} in groundwater. In other words, bedrock weathering, marine aerosol input, duration of groundwater flow (groundwater age) and evaporation cannot alone be factors in the NO_3^{2-} distribution, as these are responsible for controlling the levels of other dissolved species. Some combination of these factors may be responsible, however, there is nothing to suggest this. NO_3^{2-} is commonly found associated with organic matter, most especially human and animal wastes (Baloyi & Diamond, 2019). As the area is used for stock farming (sheep mostly), the high NO_3^{2-} levels are not surprising, given the aridity will prevent dilution, and the aridity in combination with the low topographic gradients will prevent flushing of groundwater. The random distribution of NO_3^{2-} relative to any other water quality parameters is acceptable given that the distribution of stock densities and activities, such as feedlot areas and kraals (overnight camps), are unrelated to any of the other groundwater hydrochemistry processes.

The distribution of NO_3^- is shown in Figure 10, which reveals two trends. Firstly a generally high abundance in the boreholes of catchment D53G, and secondly a more erratic distribution everywhere else. In particular are pockets of high values dotted around, suggesting very local sources, such as animal feeding or watering points where faeces and urine may be abundant enough to seep through the vadose zone and enter the groundwater. The broad area of high values in D53G are possibly related to hydrogeological controls, such as a shallow water table, highly porous vadose zone, or low hydraulic gradients, all of which may contribute to elevating nitrogen levels. Correlations with other hydrochemical parameters are poor, so evidence for one or the other processes is lacking.

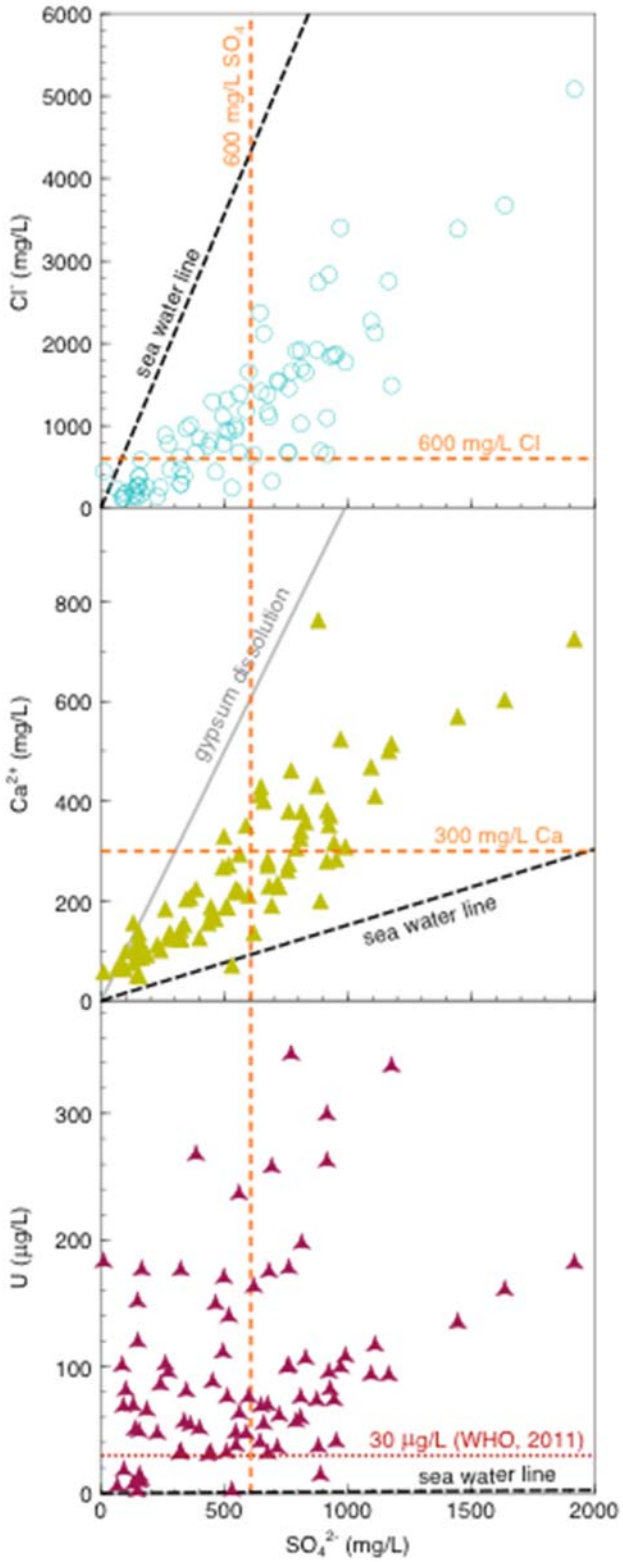

Figure 12: Scatter plots of Cl^- and Ca^{2+} versus SO_4^{2-}, with the sea water line showing a mixing line between sea water and pure water and the gypsum dissolution line for progressive dissolution of gypsum into pure water.

Before examining some of the relationships with U, it is instructive to look at the behaviour of SO_4^{2-}. The relationship between SO_4^{2-} and Cl^- (Figure 12) reveals that SO_4^{2-} is enriched in the groundwater relative to the marine Cl^- - SO_4^{2-} ratio. This must partly be due to addition of sulphur from weathering of sulphide minerals, but is probably also due to precipitation of the less soluble sulphate minerals as water evaporates, whilst Cl^- remains in solution and is flushed out of the system. The excellent correlation between Cl^- and SO_4^{2-} shows that evaporative concentration acts on both parameters, as Cl^- is a proxy for salinity (TDS-Cl^- coefficient of correlation r = 0.88). The graph of Ca^{2+} - SO_4^{2-} shows that retention of SO_4^{2-} in the system is not solely due to precipitation of gypsum. Other factors could be addition of SO_4^{2-} from weathering of sulphides, or precipitation of other secondary sulphate minerals, aside from gypsum. The graph of U against SO_4^{2-} is particularly interesting. There are two quite distinct trends in the data, unlike any of the other hydrochemistry correlations found for other parameters in this study. Both trends show increasing U concentration, but one with very little concomitant increase in SO_4^{2-} and the other with a strong associated increase in SO_4^{2-}. This suggests at least two processes operating to cause increased U concentrations, and fairly independently, as the trends have a clear separation. This will be discussed further a few paragraphs down.

This study area has high U levels in the groundwater, with 88% of samples being over the WHO (2011) limit of 30 ug/L (Table 1 & Figures 11 & 12). "High" U levels in groundwater are reported from other parts of the world, but are usually at lower levels than in this study, such as from Germany (Banning et al, 2013) and India (Duggal et al, 2017), including some studies on areas adjacent to U mining and processing, as in India (Rana et al, 2016), although other mining areas predictably reported much higher U values, such as from Namibia (Abiye & Shaduka, 2017) or Johannesburg, South Africa (Winde & Van der Walt, 2004). The high U levels found in this study are not clearly related to any of the bedrock geology. This is likely due to the complexity of U geochemistry, where it exists in different oxidation states and can precipitate as many different secondary minerals, typically being hydrous vanadates or phosphates of sodium, magnesium, potassium or calcium. The presence or absence of these elements, in particular the relatively rare vanadium or phosphorus, control the mobility of U and its migration through the landscape, including the groundwater (Post et al, 2017).

Figure 13 shows the relationships between U and selected other parameters in the groundwater. The relationship with TDS shows a big difference between the exceedances of the WHO (2011) and SANS (2001) guidelines. For TDS, about two-thirds or half exceed these respective limits, whereas U shows almost 90% of samples exceeding the WHO limit. The picture is similar for Na^+, and even more dramatic for Pb, where the limit (10 ug/L) is even outside the graph area. The enrichment of U is also evident in Figure 12, where the sea water line for U-SO_4^{2-} is barely visible in the graph, showing how much additional U there is, relative to a major ion, given that substantial marine aerosol input occurs, as evidenced by generally high Cl^- values. The

groundwater in the study area is clearly extremely enriched in U. This indicates that either the geology is particularly U rich, or there are secondary processes unique to U that cause it to become far more elevated than most of the other elements.

The four parameters plotted against U all represent different aspects of hydrogeochemistry: TDS is the total salinity, Na^+ represents the major ions, Li is a light lithophile element associated with felsic igneous rocks and silicate minerals, and Pb is a heavy siderophile element associated with ore deposits and sulphide minerals. It is therefore highly significant that all four graphs show a double pronged trend: firstly, there is a trend of rising U correlating with rising of the other parameters (*correlated U increase*), and secondly where the other parameter remains more steady with rising U (*solo U increase*). Notably, the latter is where the highest U values are found. The same double-pronged trend was noted in the U-SO_4^{2-} graph in Figure 12. Two separate processes are therefore invoked to describe these observations. The *correlated U increase* is possibly associated with evaporation, where all dissolved species increase in concentration. The *solo U increase* must be related to U-specific factors, such as originally elevated bedrock U concentrations, or conducive geochemical conditions for the enrichment of U (perhaps as secondary mineral formation in the Cenozoic sediments) in the groundwater. Importantly, it is the *solo U increase* process or processes that lead to the highest levels of U and therefore control the potability of the groundwater from a U perspective.

Returning to the map of U distribution (Figure 11), high U concentrations are confined to two general areas. These are both underlain by Cenozoic sediments and bedrock of the Bushmanland Subprovince. However, this latter group contains a wide range of rock types and so it is a little unclear how strongly the bedrock geology is controlling the U distribution, although it seems clear that bedrock geology has some part to play, given the low U concentrations over other areas. Aside from bedrock controlling the source, the extreme enrichment of U over other elements points to U being held back in the catchments when other ions are flushed out. Precipitation of secondary U minerals, a well known occurrence in arid areas (Gross & Ilani, 1987), including here in Namakwaland (Cole, 1998), provides a suitable mechanism where U levels can increase over other ions. Importantly, the complexity of secondary U minerals and their formation is likely to lead to a distribution of U in the landscape, and in turn in the groundwater, that is highly complex and not simply related to bedrock geology or one or two simple hydrochemical factors (Khoury et al, 2014).

In summary, the U distribution and correlations give it a unique signature amongst all the other hydrochemical parameters. The most plausible reasons for this include source rock control, evaporative concentration and retention within the catchment through precipitation of secondary U-bearing minerals.

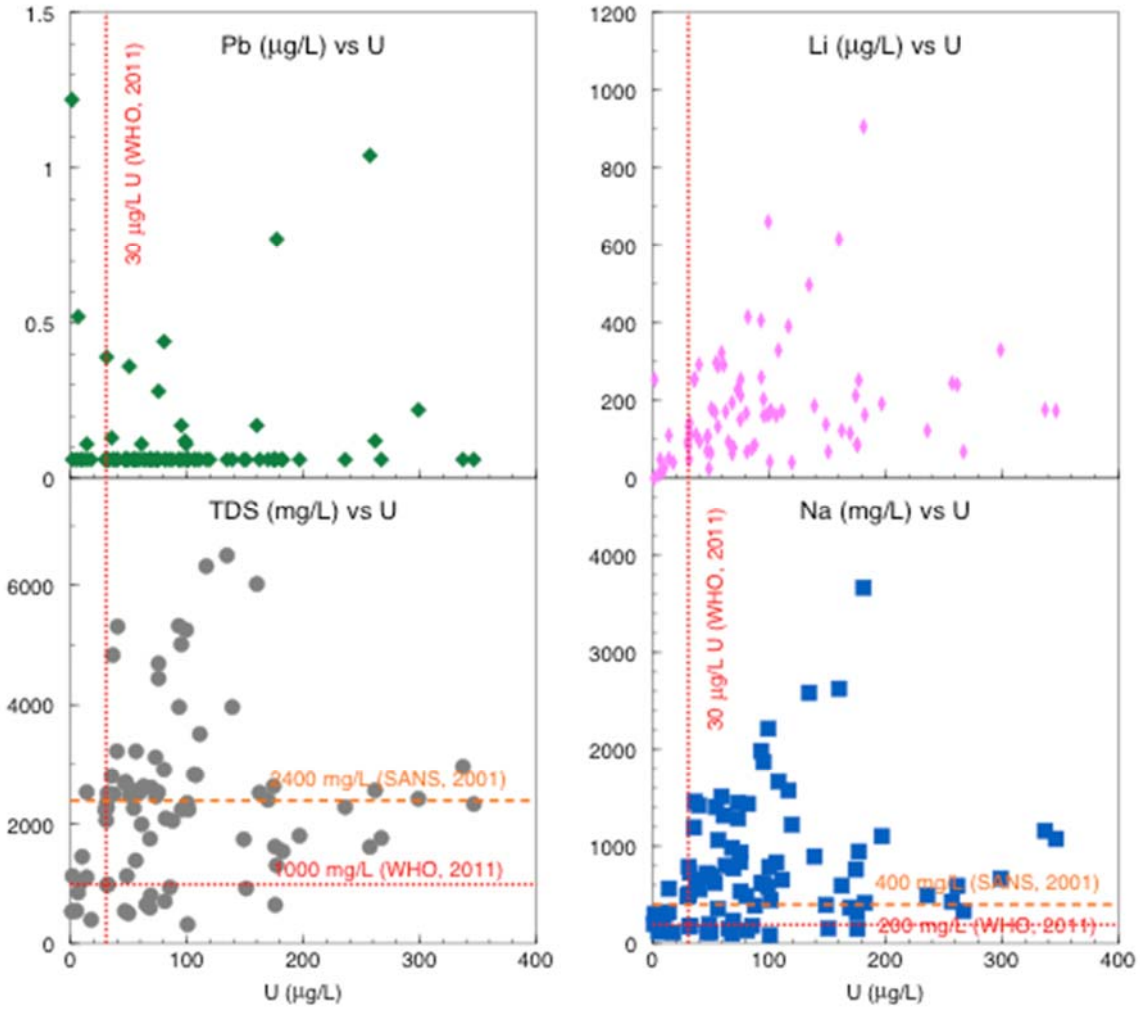

Figure 13: Relationships between U and TDS, Na, Li and Pb, with drinking water quality limits indicated where possible. The Li and Pb limits are beyond the graphs.

7 Conclusions

Groundwater in the study area has neutral to alkaline pH. The water ranges from fresh to sea water salinity, but is mostly brackish with a mean TDS of 2500 mg/L. The major ions Cl^-, Na^+ and SO_4^{2-} dominate, with lesser Ca^{2+} and HCO_3^-. Most of the water is a Na-Cl water type with a minor trend towards Ca-HCO_3. The Na-Cl type includes the higher salinity waters, suggesting evaporative enrichment as the main process responsible for creating saline groundwater.

Na^+, Mg^{2+} and K^+ are all well correlated with Cl^-, and plot close to a seawater-freshwater mixing line, suggesting much of the dissolved content in groundwater is originally from marine aerosol. Ca^{2+}, however, is highly enriched relative to the seawater mixing line, suggesting addition from rock weathering, and the excellent correlation with Cl^- again points to evaporative enrichment in addition to rock weathering. Extreme evaporative enrichment, where NaCl is precipitating from

solution, but Mg^{2+} and K^{+} salts (bittern salts) remain in solution and are flushed away, is indicated by some samples having relatively low Mg^{2+} and K^{+} compared to Cl^{-}. This is supported by the presence of salt pans in the area and the name of the Sout ("Salt') River.

Various tests of irrigation suitability were conducted with the data. Results show that salinity hazard (EC) and sodium absorption ratio (SAR) are generally good, Kelly's Ratio (KR) is marginal and the soluble sodium percentage (SSP) is generally unsuitable. Overall, the water is usable for irrigation or stock water, but in limited quantities, in select areas, for particular crops and on certain soils only.

NO_3^{2-} is generally below drinking water guidelines, but is high in some places. Lack of correlation with geology or other dissolved ions points to farm animals as the source. F^{-} is mostly above drinking water limits, but the worst values are geographically confined, showing source geology, in combination with alkaline and saline groundwater as the causes of the issue. The high salinity is largely a function of low rainfall, low topographic gradients and high evaporation in a hot, dry climate.

U is almost always above the water quality guideline limits. The distribution is unrelated to bedrock geology and hydrochemical analysis reveals two enrichment trends: one, a *correlated U increase* related to evaporation where U and other dissolved species all get concentrated; two, a *solo U increase* caused by precipitation of secondary U minerals and resulting in very high U in groundwater, poorly related to other dissolved species.

Salinity, NO_3^{2-} and F^{-} are minor to moderate hazards in the region and are quite site specific. U, however, is a widespread hazard and warrants further investigation into the water usage and the movement of U into plants and animals and possible cumulative exposure to plants, animals and humans, from soil, water, food and air. Overall, the hydrochemistry of the region is complex and opportunities exist for more detailed hydrochemical investigation that applies other techniques as well, to understand the evolution of groundwater composition.

8 Acknowledgements

The Council for Geoscience for funding the study. Farmers in the region for giving access to the land and water.

9 References

Abiye TA, Bybee G and Leshomo J 2018 Fluoride concentrations in the arid Namaqualand and the Waterberg Groundwater, South Africa: Understanding the controls of mobilization through

hydrogeochemical and environmental isotopic approaches. *Groundwater for Sustainable Development* **6**, 112–120.

Abiye TA and Leshomo J 2013 Groundwater flow and radioactivity in Namaqualand, South Africa. *Environmental Earth Sciences* **70**, 281–293.

Abiye TA and Shaduka I 2017 Radioactive seepage through groundwater flow from the uranium mines, Namibia. *Hydrology* **4**, 11.

Adams S, Titus R and Xu Y 2004 Groundwater recharge assessment of the basement aquifers of central Namaqualand. *Water Research Commission*, report 1093/1/04.

Bailie R, Armstrong R and Reid D 2007 The Bushmanland Group supracrustal succession, Aggeneys, Bushmanland, South Africa: Provenance, age of deposition and metamorphism. *South African Journal of Geology* **110**, 59-86.

Baloyi RS and Diamond RE 2019 Variable water quality of domestic wells emphasizes the need for groundwater quality monitoring and protection: Stinkwater, Hammanskraal, Gauteng. *WaterSA* **45**, 216-224

Banning A, Demmel T, Rude TR and Wrobel M 2013 Groundwater uranium origin and fate control in a river valley aquifer. *Environmental Science & Technology* **47**, 13941-13948.

Blignaut HJ, Van Aswegen G, Van der Merwe SW and Colliston WP 1983 The Namaqualand geotraverse and environs: part of the Proterozoic Namaqua Mobile Belt. *Geological Society of South Africa, Special Publication* **10**, 10-29.

Cole DI 1998 Uranium. In: Wilson MG and Anhaeusser CR (editors) *The Mineral Resources of South Africa*, 6th edition, Council for Geoscience, p642-658.

Cornell DH, Pettersson Å, Whitehouse MJ and Scherstén A 2009 A new chronostratigraphic paradigm for the age and tectonic history of the Mesoproterozoic Bushmanland ore district, South Africa. *Economic Geology* **104**, 385-404.

Davis CL, Hoffman MT, Roberts W 2016 Recent trends in the climate of Namaqualand, a megadiverse arid region of South Africa. *South African Journal of Science* **112**, 1-9.

De Brito Neto RT, Santos CA, Mulligan K and Barbato L 2016 Spatial and temporal water-level variations in the Texas portion of the Ogallala Aquifer. *Natural Hazards* **80**, 351-365.

Desmet PG and Cowling R 1998 The climate of the Karoo: A Functional Approach. In: Dean W, Milton S (editors) *The Karoo. Ecological Patterns and Processes.* Cambridge University Press, Cambridge, p3–16.

Diamond RE, Dippenaar MA and Adams S 2019 South African Hydrostratigraphy: A conceptual framework. *South African Journal of Geology* **122**, 269-282.

Doneen LD 1964 Notes on water quality in agriculture. Water science and engineering paper 4001, Department of Water Science and Engineering, University of California.

Duggal V, Sharma S, Saini K and Bajwa BS 2017 Assessment of carcinogenic and non-carcinogenic risk from exposure to uranium in groundwater from western Haryana, India. *Journal of the Geological Society of India* **89**, 663-668.

Ebrahim GY, Villholth KG and Boulos M 2019 Integrated hydrogeological modelling of hard-rock semi-arid terrain: supporting sustainable agricultural groundwater use in Hout catchment, Limpopo Province, South Africa. *Hydrogeology Journal* **27**, 965-981.

Femitha RD and Vaithyanathan C 2013 Studies on the fertilizer value of bittern from salt pans as solid fertilizer. *Asian Journal of Research in Chemistry* **6**, 1099-1102.

Foster SS and Chilton PJ 2003 Groundwater: the processes and global significance of aquifer degradation. *Philosophical Transactions of the Royal Society of London* **358**, 1957-1972.

Gobin A, Sparks D, Okedi J, Armitage N and Ahjum F 2019 Assessing the energy and carbon footprints of exploiting and treating brackish groundwater in Cape Town. *Water SA* **45**, 63-74.

Gross S and Ilani S 1987 Secondary uranium minerals from the Judean Desert and the northern Negev, Israel. *Uranium* **4**, 147-158.

Hartnady CJ, Joubert P and Stowe CW 1985 Proterozoic crustal evolution in south-western Africa. *Episodes* **8,** 236-244.

Hem JD 1985 *Study and Interpretation of the Chemical Characteristics of Natural Water*. USGS Water Supply Paper 2254.

Kanyerere T, Levy J, Xu Y and Saka J 2012 Assessment of microbiological contamination of groundwater in upper Limphasa River catchment, located in a rural area of northern Malawi. *Water SA* **38**, 581-595.

Kelly WP 1963 Use of Saline Irrigation Water. *Soil Science*, **95**, 355-39.

Khoury HN, Salameh EM and Clark ID 2014 Mineralogy and origin of surficial uranium deposits hosted in travertine and calcrete from central Jordan. *Applied Geochemistry* **43**, 49-65.

Krishan G, Rao MS, Kumar CP, Kumar S, Loyal RS, Gill GS and Semwal P 2017 Assessment of salinity and fluoride in groundwater of semi-arid region of Punjab, India. *Current World Environment* **12**, 34-41.

Kumar SK, Rammohan V, Sahayam JD and Jeevanandam M 2009 Assessment of groundwater quality and hydrogeochemistry of Manimuktha River Basin, Tamil Nadu, India. *Environmental Monitoring and Assessment* **159**, 341–351.

Joubert P 1986 Namaqualand – A model of Proterozoic accretion. *Geological Society of South Africa Transactions* **89**, 79-96.

Levin M 1983 Geohydrological investigations of the Vaalputs radioactive waste disposal site and environs. Nuclear Development Corporation of SA (Pty) Ltd. Republic PER-112 (GEA-404).

Macey PH, Bailie RH, Miller JA, Thomas RJ, De Beer C, Frei D and Le Roux PJ 2018 Implications of the distribution, age and origins of the granites of the Mesoproterozoic Spektakel Suite for the timing of the

Namaqua Orogeny in the Bushmanland Subprovince of the Namaqua-Natal Metamorphic Province, South Africa. *Precambrian Research* **312**, 68-98.

Manassaram DM, Backer LC and Moll DM 2006 A review of nitrates in drinking water: Maternal exposure and adverse reproductive and developmental outcomes. *Environmental Health Perspectives* **114**, 320-327.

McGrady MG, Ellwood RP, Srisilapanan P, Korwanich N, Worthington H and Pretty IA 2012 Dental fluorosis in populations from Chiant Mai, Thailand, with different fluoride exposures. *BMC Oral Health* **12**, 16.

Molwalefhe LN 2004 Geochemical evidence and origin of salinity in the shallow basinal brine from the Makgadigadi Pans Complexes, northeastern Botwana. In: Stephenson D, Shemang EM and Chaoka TR, *Water Resources of Arid Areas*, Balkema, Rotterdam, p409-415.

Nakwafila AN 2015 Salinisation source(s) and mechanism(s) in shallow alluvial aquifers along the Buffels River, Northern Cape Province, South Africa. MSc thesis, Stellenbosch University, Cape Town.

Ncube EJ and Schutte CF 2005 The occurrence of fluoride in South African groundwater: A water quality and health problem. *WaterSA* **31**, 35-40.

Olivier J and Van Heerden J 1999 The South African fog water collection project. Water Research Commission, Report 671/1/99, Pretoria.

Pietersen K, Titus R and Cobbing J 2009 Effective Groundwater Management in Namaqualand: Sustaining Supplies. Water Research Commission report TT 481/09.

Post VEA, Vassolo SI, Tiberghien C, Baranyikwa D and Miburo D 2017 Weathering and evaporation controls on dissolved uranium in groundwater - A case study from northern Burundi. *Science of the Total Environment* **607-608**, 281-293.

Ramesh K and Elango L 2012 Groundwater quality and its suitability for domestic and agricultural use in Tondiar River Basin, Tamil Nadu, India. *Environmental monitoring and assessment* **184**, 3887–3899.

Rana BK, Dhumale MR, Lenka P, Sahoo SK, Ravi PM and Tripathi RM 2016 A study of natural uranium content in groundwater around Tummalapalle uranium mining and processing facility, India. *Journal of Radioanalytical and Nuclear Chemistry* **307**, 1499-1506.

Richards LA 1954 Diagnosis and improvement of saline alkali soils: agriculture. US Department of Agriculture, vol 160, 60p, Washington DC.

SANS 2001 South African Standard 241: Drinking Water. South African Bureau of Standards, Pretoria.

Todd DK 1980 *Groundwater Hydrology*, 2nd edition. Wiley, New York, 535p.

Tredoux G and Talma AS 2006 Nitrate pollution of groundwater in southern Africa. In: Xu Y and Usher B, *Groundwater Pollution in Africa*, Taylor & Francis, London, p15-36.

Weaver JM, Cave L and Talma AS 2007 Groundwater sampling: a comprehensive guide for sampling methods. 2nd edition. Water Research Commission, Report TT303/07, South Africa.

WHO 2011 Guidelines for Drinking-water Quality. World Health Organisation, Geneva, 541p.

Wilcox LV 1955 Classification and use of irrigation waters. US Department of Agriculture, Circular No. 969, 19p., Washington DC.

Winde F and Van der Walt IJ 2004 The significance of groundwater - stream interactions and fluctuating stream chemistry on waterborne uranium contamination of streams - a case study from a gold mining site in South Africa. *Journal of Hydrology* **287**, 178-196.

Zhu JK 2002 Salt and drought stress signal transduction in plants. *Annual Reviews in Plant Biology* **53**, 247–273.

Appendix A: Table of raw data.

sample	pH	TDS ppm	Cl^- ppm	SO_4^{2-} ppm	Alk $CaCO_3$ ppm	F^- ppm	NO_3- ppm	Na ppm	Mg ppm	K ppm	Ca ppm	Fe ppm
SM001	7.33	2520	648	619	176	0.0	11.3	593	14	8	136	0.7
SM002	7.43	3960	919	518	170	2.1	14.0	895	67	27	273	2.5
SM003	7.13	6320	2128	1110	153	2.2	26.4	1574	71	24	411	4.0
SM004	7.40	5310	1869	953	153	2.4	14.8	557	14	5	284	1.3
SM005	8.42	2630	1108	681	149	0.0	16.0	762	72	19	230	1.9
SM006	7.35	2960	1486	1177	163	0.0	12.6	1160	62	16	514	1.1
SM007	7.46	2830	1647	829	130	2.3	16.2	832	39	14	359	1.4
SM008	7.53	2530	1023	809	106	4.0	0.0	837	38	13	341	11.6
SM009	7.27	2050	1290	452	217	2.6	65.2	387	64	17	177	0.8
SM010	7.44	1760	677	385	180	1.6	73.8	333	75	15	224	1.0
SM011	7.57	3120	1920	874	134	1.4	74.8	1449	58	18	432	1.7
SM012			263	149	185	2.3	16.5	1222	16	5	86	0.4
SM013	7.50	2520	1912	808	121	2.1	86.4	1513	33	16	326	1.5
SM014	8.56	2090	1843	928	87	2.7	36.4	1436	43	20	372	1.7
SM015	7.29	3220	1908	790	112	1.9	57.5	1063	29	13	306	1.5
SM016	7.51	3960	2268	1094	126	2.2	111.6	621	111	35	468	2.3
SM017	7.40	1740	436	464	272	2.8	42.6	394	51	17	164	0.8
SM018	7.46	2350	669	761	210	3.5	36.7	787	62	11	274	1.2
SM019	7.61	1385	388	337	184	2.9	33.8	356	29	11	153	0.7
SM020	7.18	2560	1094	915	287	3.0	18.2	590	99	26	382	1.8
SM021	7.30	2280	676	755	213	3.4	46.5	582	60	11	262	1.3
SM022	7.35	2400	777	498	186	1.9	203.6	366	101	14	330	1.7
SM023	7.58	1610	322	692	206	3.0	93.6	430	30	11	191	1.0
SM024	7.32	2420	651	915	212	2.8	130.3	667	40	13	280	1.4
SM025	8.12	6020	3670	1636	145	2.3	22.5	2628	80	26	603	2.8
SM025A	7.37	6500	3381	1445	344	2.9	32.6	2585	76	30	569	4.9
SM026	7.53	2800	1544	714	184	1.7	123.0	1191	78	11	234	1.4
SM027	7.27	1992	1535	722	281	1.6	104.0	1318	43	133	228	1.3
SM028	7.75	2530	690	889	316	0.9	113.9	564	136	6	200	1.2
SM029	7.62	849	219	131	370	0.8	98.6	126	34	2	156	0.9
SM030	8.01	5250	3400	970	163	2.7	34.7	2214	50	28	524	2.7
SM031	7.87	1306	1455	761	195	2.0	176.7	944	84	24	380	2.2
SM032	7.84		16510	3802	338	2.3	0.0	12803	329	93	926	5.5
SM033	7.55	2480	847	399	286	2.8	21.9	692	24	16	126	0.7
SM034	8.08	4440	1317	512	225	3.0	3.7	937	37	22	187	1.1
SM035	7.20	9980	5080	1918	216	2.4	13.2	3668	154	38	725	3.9
SM036	7.36	2460	1851	944	297	1.6	299.4	1286	125	18	317	1.9
SM037	7.34	5320	2754	1166	239	1.8	125.8	1985	166	24	501	3.8
SM038	7.36	2820	1769	990	334	3.8	57.6	1667	77	18	309	1.9
SM039	7.68	542	227	66	101	0.5	13.4	117	21	4	65	0.5
SM040	7.65	1450	583	162	101	0.7	12.6	296	40	7	116	1.0
SM041	7.94	1015	382	153	92	0.7	15.0	179	25	6	136	0.9
SM042	7.58	3220	2369	644	106	3.0	14.6	1420	95	32	413	2.7

sample	pH	TDS	Cl^-	SO_4^{2-}	Alk $CaCO_3$	F^-	NO_3^-	Na	Mg	K	Ca	Fe
		ppm	ppm	ppm	ppm	ppm	ppm	ppm	ppm	ppm	ppm	ppm
SM043	8.32	935	252	241	210	1.8	14.5	181	28	7	102	0.7
SM044	8.43	315	114	86	175	1.2	40.9	84	24	4	73	0.5
SM045	7.22	1126	242	530	50	1.2	0.0	301	33	14	71	0.5
SM046	7.33	2330	1655	770	197	1.8	19.5	1076	112	26	461	3.0
SM047	7.59	2280	677	559	218	2.6	65.9	496	62	11	220	1.6
SM048	8.31	917	267	148	231	1.8	50.7	153	43	9	118	0.8
SM049	7.98	1103	380	156	130	1.4	22.2	319	21	12	49	0.4
SM050	8.38	538	140	228	278	3.0	12.9	116	38	3	112	0.8
SM051	8.31	500	172	138	216	2.7	14.7	113	34	3	104	0.7
SM052	8.91	649	248	186	231	3.5	7.8	151	49	5	92	0.6
SM053	7.72	800	143	131	0	5.6	81.3	232	20	3	76	0.5
SM054	7.75	642	174	165	463	4.1	12.6	148	21	3	87	0.6
SM055	8.26	532	129	146	580	4.4	3.7	200	16	6	51	
SM056	7.91	592	159	91	569	2.9	21.5	100	22	5	68	0.6
SM057	7.76	1500	470	279	540	2.7	8.7	315	55	11	136	1.0
SM058	7.38	1750	1411	648	433	1.8	104.9	983	124	51	429	3.2
SM059	7.81	394	120	93	396	2.9	13.7	109	21	4	64	0.5
SM060	7.49	1127	266	154	414	1.8	13.9	195	23	4	95	0.7
SM061	7.19	2680	1180	588	573	1.7	145.6	721	122	32	352	2.4
SM062	8.05	2700	990	546	442	2.7	34.0	702	77	24	224	1.6
SM063	7.46	2350	1161	675	423	2.7	61.9	788	102	27	281	2.6
SM064	7.52	704	183	100	624	2.4	29.5	130	35	6	99	0.8
SM065	7.27	1620	464	323	631	2.1	86.8	316	71	15	143	1.2
SM066	7.64	5010	2835	923	529	2.1	43.9	1872	195	78	353	2.9
SM067	8.72	1540	446	11	740	5.9	7.4	416	74	21	58	0.5
SM068	8.12	2260	2120	659	215	2.8	1.7	1406	208	39	401	3.0
SM069	7.79	984	288	323	293	2.0	6.9	178	61	18	124	1.0
SM070	8.05	976	291	323	300	1.5	6.7	180	61	19	125	1.0
SM071	7.42	1800	1696	813	357	2.5	13.2	1102	90	24	379	3.7
SM072	7.36	2630	1385	561	223	1.9	0.6	799	106	23	294	7.0
SM073	7.58	2230	752	434	536	3.1	40.7	482	49	29	156	1.3
SM074	7.78	2510	943	508	455	2.3	104.8	726	58	21	189	1.7
SM075	7.93	2610	1374	675	359	1.9	64.1	770	128	32	272	2.3
SM076	7.35	2240	882	261	550	3.3	26.0	445	70	26	184	1.7
SM077	7.51	2240	778	273	573	3.2	53.0	620	43	19	124	1.1
SM078	7.57	2270	820	445	366	2.0	32.1	509	94	23	188	1.8
SM079	7.61	2060	622	319	575	1.8	128.7	494	50	31	124	1.2
SM080	7.52	2500	951	547	479	2.9	27.0	654	81	26	218	3.1
SM081	7.34	4830	2739	880	355	2.6	66.8	1460	243	76	763	6.1
SM082	7.92	2560	1002	362	471	2.9	58.2	622	70	32	208	1.7
SM083	8.73	4690	1651	598	375	3.2	121.0	536	89	38	211	2.0
SM084	8.22	2910	963	346	471	2.8	106.0	489	81	33	204	1.9
SM085	7.60	3510	1107	494	539	2.1	72.9	654	83	28	268	2.3

sample	Li	Be	B	V	Cr	Mn	Co	Ni	Cu	Zn	Ga	As	Se	Rb	Sr	Mo	Ag	Cd	Te	Ba	Tl	Pb	Bi	U
	ppb	ppb	ppb	ppb	ppb	ppb	ppb	ppb	ppb	ppb	ppb	ppb	ppb	ppb	ppb	ppb	ppb	ppb	ppb	ppb	ppb	ppb	ppb	ppb
SM001	122	48	820	14	6.4	3.7	2.8	8.6	6.4	26	2.4	23	49	4.2	1917	75	5.29	2.06	1.63	10.9	0.64	<0.06	0.72	162.5
SM002	186	19	1758	37	5.3	1.9	2.6	27.8	10.6	16	2.1	31	142	10.9	4070	49	5.01	1.85	3.07	20.0	1.60	<0.06	1.45	139.0
SM003	391	19	2299	59	5.9	23.9	3.1	41.9	19.6	237	2.2	43	197	5.0	6221	38	5.00	1.81	3.72	25.9	1.60	<0.06	1.45	116.7
SM004	95	48	687	12	2.7	3.2	3.0	14.5	5.7	37	2.3	23	49	3.7	3413	22	4.72	1.87	1.49	5.3	0.64	<0.06	0.72	40.4
SM005	213	48	1417	22	4.1	4.5	3.2	19.9	9.6	30	2.5	29	91	6.4	5409	43	5.11	1.98	1.94	16.6	0.64	<0.06	0.72	174.5
SM006	176	48	1274	19	4.4	6.0	3.0	12.1	7.9	64	2.5	25	85	20.5	3285	48	4.41	1.98	4.39	19.0	0.64	<0.06	0.72	337.1
SM007	161	48	1100	20	4.4	3.8	3.0	15.1	8.7	43	2.5	26	72	10.9	3744	40	4.33	1.94	2.01	17.2	0.64	<0.06	0.72	106.3
SM008	151	48	843	16	3.5	158.4	3.2	15.2	18.2	324	2.4	24	76	10.3	3536	47	4.25	1.97	2.36	12.7	0.63	<0.06	0.72	75.3
SM009	85	48	884	14	4.9	4.3	2.8	9.7	5.3	59	2.8	22	63	4.5	2268	14	4.01	1.84	1.80	32.3	0.64	<0.06	0.72	87.8
SM010	68	48	763	20	5.1	6.2	2.9	12.0	4.4	158	2.9	23	71	13.1	2449	19	4.03	1.87	1.65	36.8	0.64	<0.06	0.71	267.1
SM011	229	49	1552	38	4.4	10.8	3.2	20.5	12.7	137	2.6	32	111	64.7	5359	47	4.54	2.06	2.08	21.2	0.64	<0.06	0.72	73.1
SM012	40	48	629	12	8.1	4.0	2.6	6.1	4.1	567	3.2	21	37	2.9	1023	39	3.94	1.97	1.54	53.2	0.64	<0.06	0.72	119.6
SM013	323	23	1444	23	3.4	2.6	2.0	17.1	10.4	61	1.8	29	95	82.3	4445	51	6.32	1.57	2.35	12.8	1.47	<0.06	1.50	59.2
SM014	415	23	1723	28	4.2	2.2	2.1	18.4	13.6	59	1.8	31	116	108.6	5419	67	5.44	1.62	2.94	12.2	1.47	<0.06	1.49	81.8
SM015	289	23	1237	24	3.0	2.0	2.0	15.8	9.8	63	1.7	28	84	52.6	4148	41	4.76	1.54	2.24	8.2	1.45	<0.06	1.49	56.3
SM016	260	23	2085	34	4.0	26.9	2.6	25.6	14.7	1901	1.8	35	141	60.4	6456	41	5.04	1.69	2.57	9.8	1.48	<0.06	1.49	93.4
SM017	139	23	1224	14	7.4	5.6	1.7	9.8	4.7	852	2.0	22	54	2.9	2058	38	4.34	1.52	2.68	20.5	1.45	<0.06	1.49	148.9
SM018	167	23	2023	18	6.7	2.1	1.9	14.3	6.8	45	1.9	24	74	5.8	3128	83	4.36	1.79	2.82	19.9	1.45	<0.06	1.49	100.3
SM019	133	23	796	11	5.4	2.2	1.7	8.8	4.2	80	1.9	22	51	6.1	1775	69	4.33	1.67	2.08	20.7	1.44	<0.06	1.49	56.1
SM020	240	23	2915	30	9.4	10.2	2.2	21.4	13.8	50	2.1	28	101	3.3	5052	47	4.48	2.25	3.57	29.3	1.45	0.12	1.49	261.8
SM021	163	23	2010	19	5.3	2.5	1.9	14.4	6.6	43	1.9	24	73	5.8	2980	81	4.39	1.78	2.86	20.0	1.45	<0.06	1.49	99.1
SM022	115	23	954	17	5.1	3.9	2.1	18.6	4.2	670	2.1	26	88	9.0	3635	21	4.43	1.47	2.11	30.6	1.45	<0.06	1.49	169.7
SM023	244	23	939	16	3.5	2.4	2.1	13.2	9.9	1139	2.4	21	48	5.1	3363	59	4.40	2.64	3.01	21.9	1.45	1.04	1.41	257.3
SM024	330	23	1237	18	3.8	2.8	2.3	16.3	6.9	50	2.4	23	68	2.8	4732	58	4.39	1.82	2.73	25.2	1.45	0.22	1.41	299.0
SM025	616	23	2419	59	4.9	4.0	2.8	31.3	25.7	39	2.3	49	166	40.1	8965	53	4.64	1.82	5.16	16.1	1.46	0.17	1.42	160.2
SM025A	498	19	3303	96	8.2	9.2	3.6	53.4	30.9	276	2.1	63	229	40.7	8549	32400	5.90	1.85	4.47	21.0	1.60	<0.06	1.45	134.5
SM026	253	23	1430	33	4.7	5.8	2.3	15.5	17.4	43	2.3	32	83	46.7	3889	18	4.44	1.69	2.86	17.4	1.45	0.13	1.41	35.5
SM027	292	23	1562	32	5.4	10.8	2.2	15.9	13.2	199	2.1	31	83	47.2	3352	27	4.42	1.72	2.68	6.1	1.47	0.11	1.41	61.2
SM028	110	23	1698	21	6.0	18.2	2.4	14.8	22.4	171	2.2	25	87	8.6	3204	7	4.40	1.66	2.70	16.2	1.46	0.11	1.41	14.0
SM029	48	23	364	45	7.2	2.5	2.1	17.9	11.4	327	2.9	21	33	2.8	1270	3	4.37	2.21	1.90	48.4	1.46	0.52	1.41	6.6
SM030	661	23	1943	55	5.3	4.5	2.8	29.3	23.0	68	2.3	48	156	52.3	7088	62	4.58	2.03	3.68	19.3	1.47	0.11	1.41	99.4
SM031	252	23	1522	30	5.6	2.1	2.5	24.3	23.4	47	2.3	32	122	13.2	5406	24	4.50	1.73	3.23	18.3	1.45	0.77	1.41	177.2
SM032	3097	23	5035	211	14.9	15.2	4.3	63.9	123.1	24	3.0	170	537	100.1	21629	33	5.73	1.79	9.77	52.9	1.47	0.12	1.43	98.4
SM033	179	15	926	31	6.4	1.9	1.6	9.9	11.0	65	1.6	27	52	3.5	1540	24	5.57	1.58	1.98	12.1	1.39	0.36	1.28	50.6
SM034	254	15	1118	27	4.0	2.1	1.7	13.7	10.6	443	1.5	29	68	5.5	2638	22	5.66	1.47	2.58	4.1	1.38	<0.06	1.28	75.7
SM035	906	16	3280	97	8.0	2.2	2.9	44.9	43.6	25	1.8	73	255	82.8	12091	48	7.05	1.61	7.64	24.9	1.49	<0.06	1.28	181.3
SM036	226	16	2096	37	6.0	13.2	2.1	21.6	18.0	886	1.8	34	130	13.1	4780	21	5.28	1.49	4.77	18.0	1.38	<0.06	1.28	73.5
SM037	406	16	2218	58	6.2	19.1	2.7	35.7	23.3	238	1.8	51	160	56.8	7817	21	5.45	1.54	3.59	23.3	1.47	<0.06	1.28	93.1
SM038	329	16	2282	56	5.7	4.4	2.0	22.8	19.6	177	1.8	39	122	5.3	4411	54	5.31	1.61	3.72	20.1	1.38	<0.06	1.28	108.0
SM039	10	15	156	9	2.5	11.0	1.4	7.2	2.2	159	2.6	20	29	3.1	507	3	5.11	1.40	1.76	61.0	1.38	<0.06	1.28	5.1
SM040	26	15	306	15	3.0	13.1	1.6	10.1	3.7	146	2.6	23	49	4.9	1073	3	5.14	1.39	1.89	62.2	1.38	<0.06	1.28	10.1
SM041	17	15	192	11	2.3	15.9	1.7	11.1	2.5	53	3.4	21	39	4.2	1368	4	5.15	1.38	1.74	108.1	1.38	<0.06	1.28	8.6
SM042	292	15	1322	52	6.8	13.1	2.8	30.3	14.2	37	1.9	45	155	48.6	5574	21	5.39	1.46	2.74	27.4	1.38	<0.06	1.28	40.0

sample	Li	Be	B	V	Cr	Mn	Co	Ni	Cu	Zn	Ga	As	Se	Rb	Sr	Mo	Ag	Cd	Te	Ba	Tl	Pb	Bi	U
	ppb	ppb	ppb	ppb	ppb	ppb	ppb	ppb	ppb	ppb	ppb	ppb	ppb	ppb	ppb	ppb	ppb	ppb	ppb	ppb	ppb	ppb	ppb	ppb
SM043	77	15	319	7	2.4	1.5	1.5	8.4	3.0	26	1.8	20	38	20.2	662	7	5.11	1.40	1.82	19.3	1.38	<0.06	1.28	85.5
SM044	42	15	207	14	2.9	1.6	1.4	6.5	2.0	100	2.3	19	53	4.9	444	3	5.11	1.42	1.70	49.4	1.38	<0.06	1.28	100.8
SM045	253	15	350	6	2.3	209.7	1.4	6.6	3.6	36	1.6	19	32	66.5	313	3	5.12	1.45	1.75	10.4	1.38	<0.06	1.28	1.8
SM046	173	16	1239	35	5.3	2.5	2.4	34.2	10.3	23	1.7	38	143	25.6	4809	51	5.29	1.62	3.29	19.6	1.38	<0.06	1.28	346.5
SM047	123	16	765	15	3.8	8.5	1.8	19.2	6.5	27	1.5	24	64	20.6	1444	34	5.14	1.71	2.70	4.0	1.38	<0.06	1.28	236.1
SM048	68	15	248	9	3.5	4.6	1.6	15.1	4.3	308	2.4	20	32	8.4	470	31	5.12	1.62	1.82	51.8	1.38	<0.06	1.28	150.9
SM049	50	15	601	13	3.5	3.7	1.4	5.3	3.3	22	2.2	21	46	7.8	818	10	5.13	1.41	2.15	42.7	1.38	<0.06	1.28	13.9
SM050	70	15	347	4	3.0	6.1	1.5	10.7	2.1	29	1.5	18	28	6.9	466	6	5.11	1.38	1.92	4.8	1.51	<0.06	1.28	46.8
SM051	65	15	272	5	3.7	2.1	1.5	9.2	3.3	54	1.6	19	29	4.6	434	13	5.11	1.42	1.79	11.5	1.43	<0.06	1.28	50.0
SM052	93	15	351	7	3.6	2.4	1.5	8.3	3.8	10	1.8	19	33	6.0	532	15	5.12	1.43	1.70	21.2	1.43	<0.06	1.28	65.1
SM053	79	15	625	24	4.5	1.3	1.6	7.8	3.1	26	1.6	20	31	1.7	627	16	5.66	1.36	2.12	17.4	1.22	<0.06	1.27	69.0
SM054	84	15	292	7	2.0	10.8	1.7	9.0	2.3	241	1.2	19	28	2.8	361	25	5.36	1.41	1.40	<0.31	1.22	<0.06	1.26	176.0
SM055	<0.22	54	15	5540	7.3	3.0	389.1	1.5	5.9	<3.6	8.8	2	19	25.7	6	371	19.15	5.11	<0.04	1.6	<0.06	1.22	<0.01	1.3
SM056	64	15	341	6	3.7	4.2	1.7	8.6	2.0	163	1.3	20	29	2.2	537	12	5.08	1.36	1.52	2.4	1.22	<0.06	1.26	68.4
SM057	129	15	830	13	3.8	2.3	1.8	12.8	3.4	74	1.7	23	61	18.5	1082	64	5.43	2.00	1.89	23.0	1.29	<0.06	1.27	5123.
SM058	194	15	2018	44	5.6	3.0	2.7	37.0	9.3	53	2.1	41	141	8.3	4796	15	6.38	1.37	2.91	47.2	1.22	<0.06	1.27	68.4
SM059	40	15	334	8	2.8	1.9	1.6	7.0	2.6	87	1.3	20	28	1.7	458	16	4.77	1.37	1.56	3.6	1.22	<0.06	1.27	17.8
SM060	24	15	242	11	3.8	10.5	1.8	12.3	3.7	686	2.5	21	35	1.9	581	8	4.80	1.38	1.51	61.8	1.22	<0.06	1.27	48.5
SM061	105	15	1397	33	6.3	2.0	2.5	31.7	6.9	12	1.7	33	118	9.7	3631	7	5.22	1.33	2.15	23.8	1.22	<0.06	1.27	46.9
SM062	109	15	1480	24	4.6	1.6	2.0	19.1	6.7	340	1.6	29	106	9.5	2594	21	4.97	1.40	2.60	14.3	1.22	<0.06	1.27	47.6
SM063	134	23	1980	29	5.0	81.1	3.4	33.5	10.3	1241	2.3	32	137	8.6	3535	18	6.02	1.74	3.51	17.0	1.58	0.39	1.67	31.1
SM064	68	23	491	9	4.8	4.3	2.3	12.0	2.9	89	2.2	22	38	1.8	755	14	4.78	1.69	2.20	10.7	1.58	<0.06	1.66	81.2
SM065	87	23	943	23	4.8	2.3	2.3	16.7	5.4	18	2.5	26	75	10.2	1558	17	4.94	1.79	2.64	29.1	1.58	<0.06	1.66	175.7
SM066	203	23	3599	80	15.0	3.7	3.1	38.6	22.7	16	2.6	59	272	26.8	6617	22	6.60	1.72	4.54	34.7	1.58	0.17	1.67	95.3
SM067	163	23	1381	18	6.9	2.5	2.1	10.0	7.0	10	2.1	26	61	27.3	1078	34	4.79	1.77	2.98	5.7	1.58	<0.06	1.66	182.3
SM068	298	23	1611	62	6.9	42.4	3.4	37.4	15.5	568	2.7	55	189	20.7	5345	13	5.43	2.18	3.87	41.1	1.58	<0.06	1.67	54.5
SM069	112	23	443	13	3.7	4.4	2.2	16.3	3.1	1431	2.3	25	41	23.9	482	5	4.71	1.69	2.96	17.5	1.59	<0.06	1.67	32.2
SM070	114	23	439	11	3.7	60.9	2.5	16.7	3.4	1498	2.3	24	41	23.9	468	5	4.70	1.67	2.68	17.4	1.59	<0.06	1.66	31.6
SM071	192	23	1204	42	5.8	20.3	3.4	34.4	11.5	1310	2.5	41	151	37.6	4519	46	4.93	1.88	7.30	26.0	1.58	<0.06	1.67	196.9
SM072	171	23	1077	39	5.1	133.8	4.0	28.0	9.0	297	2.5	35	122	24.0	3207	16	4.85	1.79	3.96	27.6	1.59	<0.06	1.66	62.9
SM073	93	20	1705	18	4.1	7.3	2.2	15.1	6.1	131	1.4	23	87	7.6	2005	19	6.72	1.56	2.93	2.9	1.15	<0.06	1.13	29.9
SM074	143	20	1679	26	4.2	6.0	2.3	19.0	8.1	82	1.7	27	113	12.9	2365	20	5.98	1.55	3.22	17.8	1.14	<0.06	1.13	31.9
SM075	79	20	1421	35	4.8	9.2	2.6	26.8	8.1	122	1.8	33	153	12.9	3965	9	5.83	1.51	2.67	22.3	1.14	<0.06	1.13	69.4
SM076	174	20	1057	25	4.5	5.1	2.2	18.5	5.4	201	1.5	26	91	8.2	2167	12	5.03	1.53	2.33	9.7	1.14	<0.06	1.13	101.7
SM077	161	20	1429	23	5.7	1.6	2.0	12.8	6.6	183	1.4	26	85	7.4	1446	25	4.96	1.82	2.68	1.2	1.14	<0.06	1.13	95.5
SM078	48	20	1046	24	4.2	13.3	2.3	17.4	6.1	352	1.7	26	102	10.5	2357	5	4.95	1.52	2.21	19.0	1.14	<0.06	1.13	31.5
SM079	82	20	1173	22	4.2	8.6	2.1	12.6	6.0	193	1.6	24	77	9.9	1723	15	4.83	1.54	2.28	12.6	1.14	<0.06	1.13	30.9
SM080	112	20	1700	26	4.5	48.8	2.6	22.2	7.6	2873	1.7	27	114	11.1	2601	18	4.92	1.59	7.40	16.0	1.14	<0.06	1.14	37.3
SM081	255	20	2808	76	7.6	63.8	4.8	70.6	17.7	860	2.1	65	353	19.2	1087	8	5.74	1.53	7.99	43.6	1.14	<0.06	1.13	36.4
SM082	170	20	1394	33	5.4	2.4	2.3	19.9	7.4	73	1.6	30	113	12.3	2575	19	4.80	1.66	3.19	10.6	1.14	<0.06	1.13	53.6
SM083	213	19	2074	42	5.7	4.2	2.4	22.7	12.4	56	2.0	35	155	22.5	3456	22	3926.6	1.74	3.15	18.8	1.60	0.28	1.45	75.7
SM084	167	19	1174	29	5.1	11.4	2.4	22.0	6.5	415	1.9	29	105	8.4	2593	9048	4.98	1.69	2.56	10.8	1.60	0.44	1.45	80.5
SM085	173	19	1609	33	5.0	2.8	2.6	26.8	8.3	133	1.8	31	108	6.8	2792	6432	4.94	1.71	3.06	5.9	1.60	<0.06	1.45	111.2